JIPB Journal of Integrative Plant Biology

Research Article
https://doi.org/10.1111/jipb.70111

Plastid and nuclear phylogenomics of *Cyphostemma* (Vitaceae) provide new insights into genome size evolution across sub-Saharan Africa

Rindra M. Ranaivoson[1,2,3,4†], Romer N. Rabarijaona[1,2†], Jin-Ren Yu[1,2,3], Yi-Chen You[1,2,3], Russell L. Barrett[5,6], Ju Zhou[1,2,3], Bing Liu[1,2,7], Wyckliffe Omondi Omollo[1,2], Chuan-Yu Du[1,2,3], Da-Ming Zhang[1,2], Mijoro Rakotoarinivo[4], Jie Cheng[1,2,8], Chao-Bin Li[1,2], Yang Dong[1,2], Ilia J. Leitch[9], Alexandre Antonelli[9,10,11,12], Jun Wen[13], Zhi-Duan Chen[1,2,7*] and Li-Min Lu[1,2*]

1. State Key Laboratory of Plant Diversity and Specialty Crops & Key Laboratory of Systematic and Evolutionary Botany, Institute of Botany, The Chinese Academy of Sciences, Beijing 100093, China
2. China National Botanical Garden, Beijing 100093, China
3. University of Chinese Academy of Sciences, Beijing 100049, China
4. Department of Plant Biology and Ecology, Faculty of Sciences, University of Antananarivo, Antananarivo BP 906, Madagascar
5. National Herbarium of New South Wales, Australian Botanic Garden, Mount Annan 6002, Australia
6. Evolution and Ecology Research Centre, School of Biological, Earth, and Environmental Sciences, University of New South Wales, Kensington 2052, Australia
7. Sino-Africa Joint Research Center, The Chinese Academy of Sciences, Wuhan 430074, China
8. Department of Computational and Systems Biology, John Innes Centre, Norwich NR4 7UH, UK
9. Royal Botanic Gardens, Kew, Richmond, Surrey TW9 3AB, UK
10. Department of Biological and Environmental Sciences, Gothenburg Global Biodiversity Centre, University of Gothenburg, Gothenburg SE-41319, Sweden
11. Wuhan Botanical Garden, The Chinese Academy of Sciences, Wuhan 430074, China
12. Department of Biology, University of Oxford, Oxford OX1 3RB, UK
13. Department of Botany, National Museum of Natural History, Smithsonian Institution, Washington, DC 20013-7012, USA
†These authors contributed equally to this work.
*Correspondences: Zhi-Duan Chen (zhiduan@ibcas.ac.cn); Li-Min Lu (liminlu@ibcas.ac.cn, Dr. Lu is fully responsible for the distribution of all materials associated with this article)

Rindra M. Ranaivoson

Li-Min Lu

ABSTRACT

Genome size, the total amount of DNA content in the cell nucleus, varies greatly among flowering plants. One factor underlying this variation is the environment under which plants evolve. Given this premise, harsh environmental conditions in arid regions may profoundly influence genome evolution. However, the specific impact of aridification on genome size evolution, particularly for African lineages, remains largely unexplored. Here, we investigate linkages between genome size evolution and ecological adaptation using the genus *Cyphostemma* in the grape family (Vitaceae) as a model. *Cyphostemma* species exhibit genome size expansion and remarkable morphological traits in arid environments, including succulent stems or leaves and loss of tendrils. Our biogeographic reconstruction, based on substantial taxon sampling (112 of 200 species), reveals that *Cyphostemma* originated in continental Africa during the late Eocene to Oligocene and has undergone rapid radiation since the middle Miocene, coinciding with intensified aridification and geological activity in eastern Africa. Incorporating extensive data on traits, habitats, genome size, and chromosome numbers, we show that *Cyphostemma* species with the largest genomes are succulent polyploids restricted to nutrient-rich limestone outcrops. Broad-scale analyses across eudicots further confirm

that larger genomes are significantly associated with both succulence and arid habitats. Our findings reveal a strong association between genome size expansion, polyploidy, and adaptive traits, indicating that genome size is a hitherto neglected trait associated with the radiation of succulent plants during the African aridification in the Cenozoic.

Keywords: aridification, *Cyphostemma*, diversification, ecological adaptation, genome size

Ranaivoson, R. M., Rabarijaona, R. N., Yu, J.-R., You, Y.-C., Barrett, R. L., Zhou, J., Liu, B., Omollo, W. O., Du, C.-Y., Zhang, D. M., et al. (2026). Plastid and nuclear phylogenomics of *Cyphostemma* (Vitaceae) provide new insights into genome size evolution across sub-Saharan Africa. J. Integr. Plant Biol. **00:** 1–22.

INTRODUCTION

The vast diversity of flowering plants (angiosperms), comprising some 345,861 documented species (World Flora Online Plant List, https://wfoplantlist.org/; accessed in September 2025), is characterized by another remarkable yet less understood diversity within their cells: genome size. Ranging ~2,400-fold, from 1C-values = 0.063 pg in the carnivorous plant *Genlisea aurea* A.St.-Hil. (Fleischmann et al., 2014) to 152.23 pg in the monocot *Paris japonica* (Franch. & Sav.) Franch. (Pellicer et al., 2010), angiosperms exhibit the largest genome size range of any comparable major lineage of organisms (Faizullah et al., 2021; Henniges et al., 2023). This variation has profound ecological and evolutionary implications (e.g., Carta et al., 2020; Roddy et al., 2020; Guo et al., 2024). Species with small genomes (e.g., *Arabidopsis thaliana* (L.) Heynh., 1C-value = 0.16 pg) commonly exhibit broad geographic ranges and ecological plasticity, enabling successful competition and occupation of diverse niches (Zenil-Ferguson et al., 2016; Simonin and Roddy, 2018; Pyšek et al., 2023; Šmarda et al., 2023). By contrast, species with large genomes (e.g., *Trillium rhombifolium* Raf., 1C-value = 111.50 pg) often have restricted distributions (Bureš et al., 2024), a pattern consistent with the large genome constraint hypothesis that posits ecological filtering against high DNA content (Knight et al., 2005).

Genome size dynamics reflect a balance between DNA gain and loss. Expansion occurs primarily through polyploidization (whole genome duplication (WGD)) and repetitive DNA amplification. In contrast, contraction is primarily achieved through DNA recombination-based mechanisms that result in DNA loss. These deletion processes, ranging from small-scale events (e.g., < 100 bp, via illegitimate recombination; Devos et al., 2002) to large-scale deletions (kb–Mb, via various double-strand break repair pathways; Schubert and Vu, 2016), are often activated during post-WGD diploidization and lead to genome downsizing, predominantly through transposable element removal (e.g., Dodsworth et al., 2016; Escudero and Wendel, 2020; Wang et al., 2021). Notably, although all angiosperms are derived from polyploid ancestors (Wendel, 2015; Landis et al., 2018), and many lineages have accumulated repetitive elements (Novák et al., 2020), most species maintain relatively small genomes (i.e., mode for 10,770 species is 1C = 0.60 pg; Henniges et al., 2023).

Extensive research on the biological significance of genome size diversity has primarily focused on the nucleotypic theory (Bennett, 1971), which posits that genome size imposes biophysical constraints at the nuclear and cellular levels. These constraints influence functional traits and phenotypes independently of the encoded DNA sequences. For example, a large genome requires a larger nucleus and cell (Beaulieu et al., 2008) and extends the minimum duration of the cell cycle. Support for the nucleotypic theory includes the study by Šímová and Herben (2012), who analyzed 269 herbaceous angiosperm species from 46 families and found that genome size scales positively with nuclear and cell volume, as well as with the durations of S-phase of the cell cycle and hence the whole cell cycle. These nucleotypic relationships have a direct influence on morphological and physiological traits. For example, Beaulieu et al. (2008) showed that a larger genome leads to larger guard cells in a study of 101 angiosperm species, impacting water and gas exchange and influencing water-use efficiency, photosynthesis, and growth rates (Roddy et al., 2020; Šmarda et al., 2023; Simpson et al., 2024). Consequently, genome size affects where and how species can grow and compete. In addition, the increased nutrient demands (especially for nitrogen and phosphorous) of cells with larger genomes can limit competitiveness in nutrient-poor soils, as shown by field experiments such as those by Guignard et al. (2016) in south-east England, UK, Peng et al. (2022) in Inner Mongolia, and Morton et al. (2024) across North America and Europe. Ultimately, these cellular constraints scale up to influence plant ecology, evolution, and global distribution (e.g., Bureš et al., 2024). These data highlight a fundamental trade-off: While larger genomes can incur costs, such as slower cell division and reduced growth rates, and are more restricted in their distribution, the process of repeat amplification that enlarges genomes may, under certain conditions, provide adaptive benefits by rapidly generating genetic variation upon which selection can act. For instance, transposable element activity can create adaptive variation for stress and pathogen resistance (e.g., in rice), while whole-genome duplications, which at least initially lead to larger genomes, often confer broad-spectrum stress resilience across diverse lineages through genomic buffering and regulatory flexibility (Casacuberta and González, 2013; Van de Peer et al., 2021). Therefore, species with larger genomes may not always be poor competitors in natural landscapes (Bomblies, 2020; Théroux-Rancourt et al., 2021; Ebadi et al., 2023; Šmarda et al., 2023).

Challenging environmental conditions in arid regions may act as critical constraints on genome size evolution. However, the mechanisms linking genome size and xeric

adaptation are complex and can be context-dependent. Comparative studies across numerous families (e.g., Asteraceae, Poaceae, and Ranunculaceae) reveal contrasting adaptive strategies: Species with larger genomes may achieve greater water-use efficiency through larger stomata with lower conductance and enhanced water storage capacity in big vacuoles, whereas species with smaller genomes (e.g., Caryophyllaceae, Cyperaceae) can improve water-use efficiency under drought by rapidly adjusting stomatal architecture and closure rates (Hetherington and Woodward, 2003; Veselý et al., 2020; Pacey et al., 2022; Šmarda et al., 2023; Van Mazijk et al., 2024). The Neogene aridification, which created novel dry habitats like savannas, limestone outcrops, and deserts, may have triggered the evolution of a "succulent syndrome," potentially linked to genome size changes in arid-adapted lineages (Arakaki et al., 2011). This raises the question of whether shifts in genome size might be associated with the emergence of succulence, adaptation to drought, and/or the rapid radiations within arid regions. Testing these scenarios requires comprehensive phylogenetic comparisons among closely related species that exhibit broad genome size heterogeneity and occupy divergent habitats.

Here, we investigate the species-rich genus *Cyphostemma* (in the grape family Vitaceae), which contains ca. 200 species (Wen et al., 2018), mainly distributed in continental Africa and Madagascar, with three species in Asia (Figure 1A). The genus is well-known for its habitat diversity, spanning rainforests to rocky outcrops (Figure 1B–D), and unique morphological traits including pachycaulous (succulent bottle-shaped) trunks, tuberous roots, succulent leaves, and loss of the Vitaceae-ancestral tendrils (Figure 1E–G). These innovations may have facilitated the adaptation of *Cyphostemma* species to diverse harsh habitats across sub-Saharan Africa (Hearn et al., 2018). *Cyphostemma* also exhibits variation in ploidy level and genome size, with reported chromosome numbers ranging from $2n = 2x = 22$ to $2n = 6x = 66$ (Lavie, 1979) and genome sizes varying from 1.33 to 3.25 pg/1C (Chu et al., 2018). The largest genome so far reported for Vitaceae was in *Cyphostemma humile* (3.25 pg/1C), a species native to limestone outcrops of southern Africa, which is nearly 10 times larger than the smallest genome, in *Vitis vulpina* L. (0.31 pg/1C) (Chu et al., 2018). However, genome size data remain scarce for *Cyphostemma*, with only three species sampled to date, leaving the evolutionary significance of genome size variation in this genus poorly understood.

Although recent phylogenetic studies have recognized three major clades in *Cyphostemma*, relationships within and among these groups remain unresolved, primarily due to limitations in taxon sampling and molecular data (e.g., Rabarijaona et al., 2023, using plastome data for just 42 species; Hearn et al., 2018, using a 4 plastid + 1 nuclear dataset for 64 species; and You et al., 2024, using plastome coding sequences (CDS) + 11 plastid data for 78 species). By integrating cytological, morphological, and ecological data within a robust phylogenetic framework, the genus may serve as an ideal system for investigating genome size evolution and its role in trait diversification and ecological adaptation.

In this study, we combine newly generated shallow whole-genome sequencing data (112 species), genome size measurements (72 species), and chromosome counts (20 species) across *Cyphostemma* to investigate how genome size evolution correlates with morphological traits and ecological factors. We aim to: (i) Infer the geographic range evolution and diversification dynamics in *Cyphostemma*; and (ii) Test the evolutionary impact of habitat types, aridity levels, morphological traits, and ploidy levels on genome size evolution. Our results uncover significant variation in genome size within *Cyphostemma* and suggest that aridification and succulence are associated with the evolution of larger genomes. Using a new, robust phylogenetic framework generated here, together with extensive statistical analyses, we further compare these findings with patterns across eudicots, revealing key similarities as well as previously unrecognized idiosyncrasies.

RESULTS

Phylogeny and biogeography of *Cyphostemma*

We reconstructed the most comprehensive and robust phylogeny of *Cyphostemma* to date using both plastid and nuclear datasets, including 112 of ca. 200 recognized species (see Figure S1 for sampling locations and Materials and methods for details of the different datasets analyzed). The concatenated alignment of the 112-plastome dataset included the large single-copy (LSC), small single-copy (SSC), and inverted repeat (IR) regions, resulting in a total aligned length of 133,969 bp. The plastome trees consistently recovered three major clades with moderate to strong support, whereas the nuclear data recovered four (Figure S2). Based on the 112-plastome dataset (Figures 2, S2), clade I comprises species with pinnate leaves, mainly from Madagascar, along with one species from Mauritius, *C. mappia* (Lam.) Galet, and one from southern Africa, *C. sulcatum* (C.A.Sm.) J.J.M.van der Merwe. Notably, the newly sampled species from southern Africa, *C. sulcatum*, is sister to the rest of clade I (with a bootstrap support value BS = 77%). Clades II and III consist of species with digitate leaves. Clade II includes only two Asian species: *C. dehongense* L.M.Lu & V.C.Dang and *C. auriculatum* (Roxb.) P.Singh & B.V.Shetty. Most species in clade III occur in continental Africa, with only two exceptions from Madagascar and the Comoros archipelago (*C. sambiranense* Rabarij. & L.M.Lu and *C. glandulosopilosum* Desc.), which are sister to each other.

We detected cytonuclear discordance concerning the positions of the two Asian species and two anomalous continental African species, *C. adenocaule* (Steud. ex A.Rich.) Desc. ex Wild & R.B.Drumm. and *C. cymosum* (Schumach. & Thonn.) Desc. (Figure S2), whose phylogenetic positions were also found to be difficult to establish in previous studies (Hearn et al., 2018; Rabarijaona et al., 2023). The two Asian

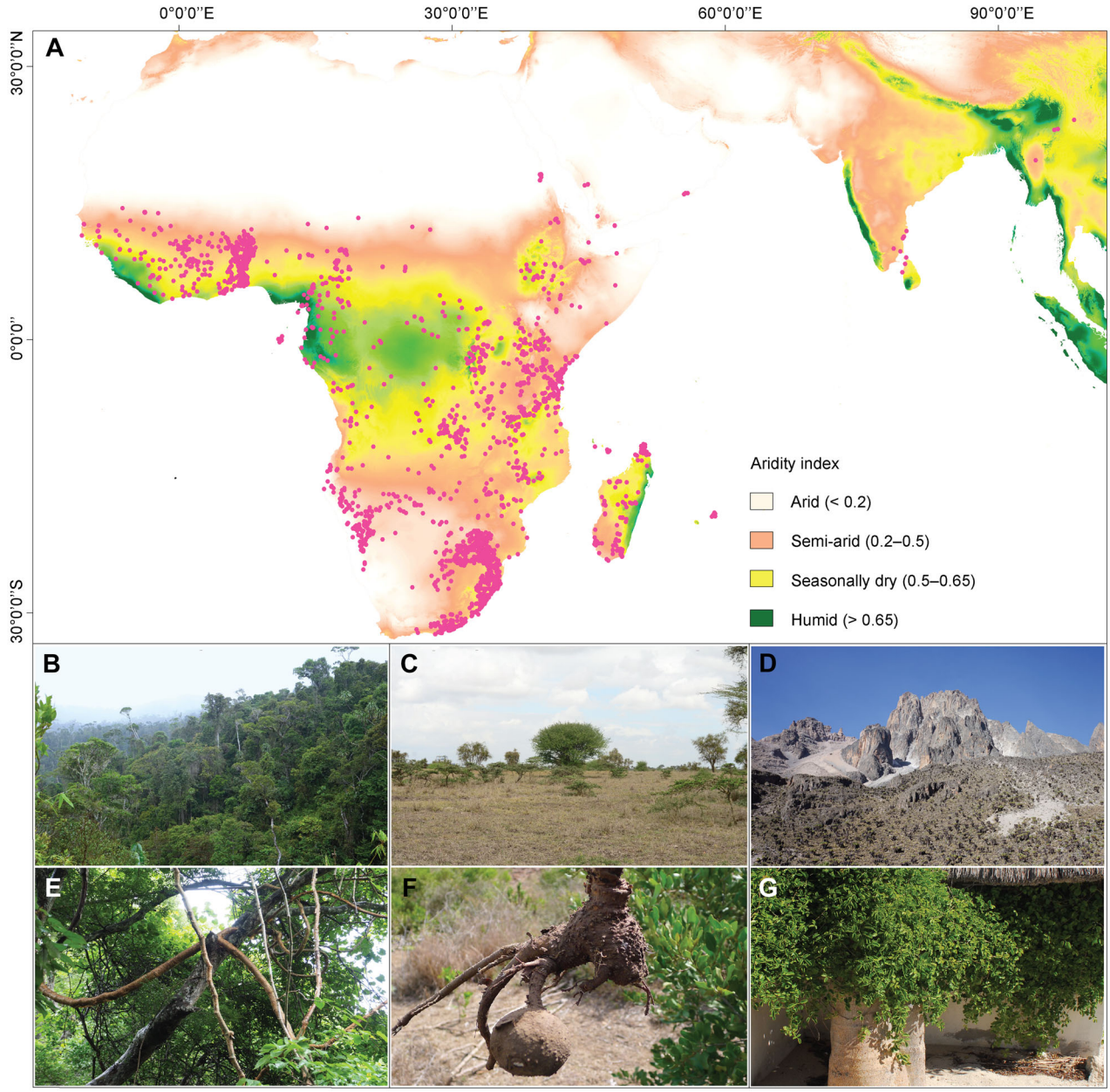

Figure 1. Distribution, major habitat types, and related adaptive traits of *Cyphostemma*
(A) Map showing the gradient of aridity index and distribution of species in *Cyphostemma* (pink dots). **(B–D)** Habitat types: rainforest **(B)**, savanna **(C)**, and rocky outcrops **(D)**. **(E–G)** Representative traits: liana **(E)**, presence of tuberous roots **(F)**, and succulent stem **(G)**. Photo credits: Bing Liu **(B, E)**, Li-Min Lu **(C)**, and Zhi-Duan Chen **(D, F, and G)**.

species formed a clade sister to clade III in both the 112-plastome and 83-plastome phylogenies (Figures 2, S2A; see Materials and methods), but this relationship was not supported in the 83taxa-229nu phylogeny (Figure S2B). Similarly, *C. adenocaule* and *C. cymosum* were inferred as an early divergent lineage of clade III in the plastome phylogenies (Figures 2, S2A), but they were sister to the remaining *Cyphostemma* taxa in the nuclear phylogeny (Figure S2B).

We estimated the crown age of *Cyphostemma* to be in the Oligocene (26.87 Ma, 95% highest posterior density (HPD): 20.11–32.51 Ma) to late Eocene (36.63 Ma, 95% HPD, 23.11–48.98 Ma) based on the 159-plastome and the 104taxa-229nu datasets, respectively (Figures S3, S4). This discrepancy in divergence times between the two datasets may be partially explained by the larger taxon sampling of the plastid dataset, but more likely results from the slower nucleotide substitution rates in plastid genes compared to nuclear genes (Okuyama et al., 2005; Dong et al., 2022).

The best model for biogeographic reconstruction was BAYAREALIKE + j (Table S1). Our biogeographic reconstruction suggests that *Cyphostemma* most likely originated in tropical Africa (Figure 2). The genus subsequently dispersed to southern

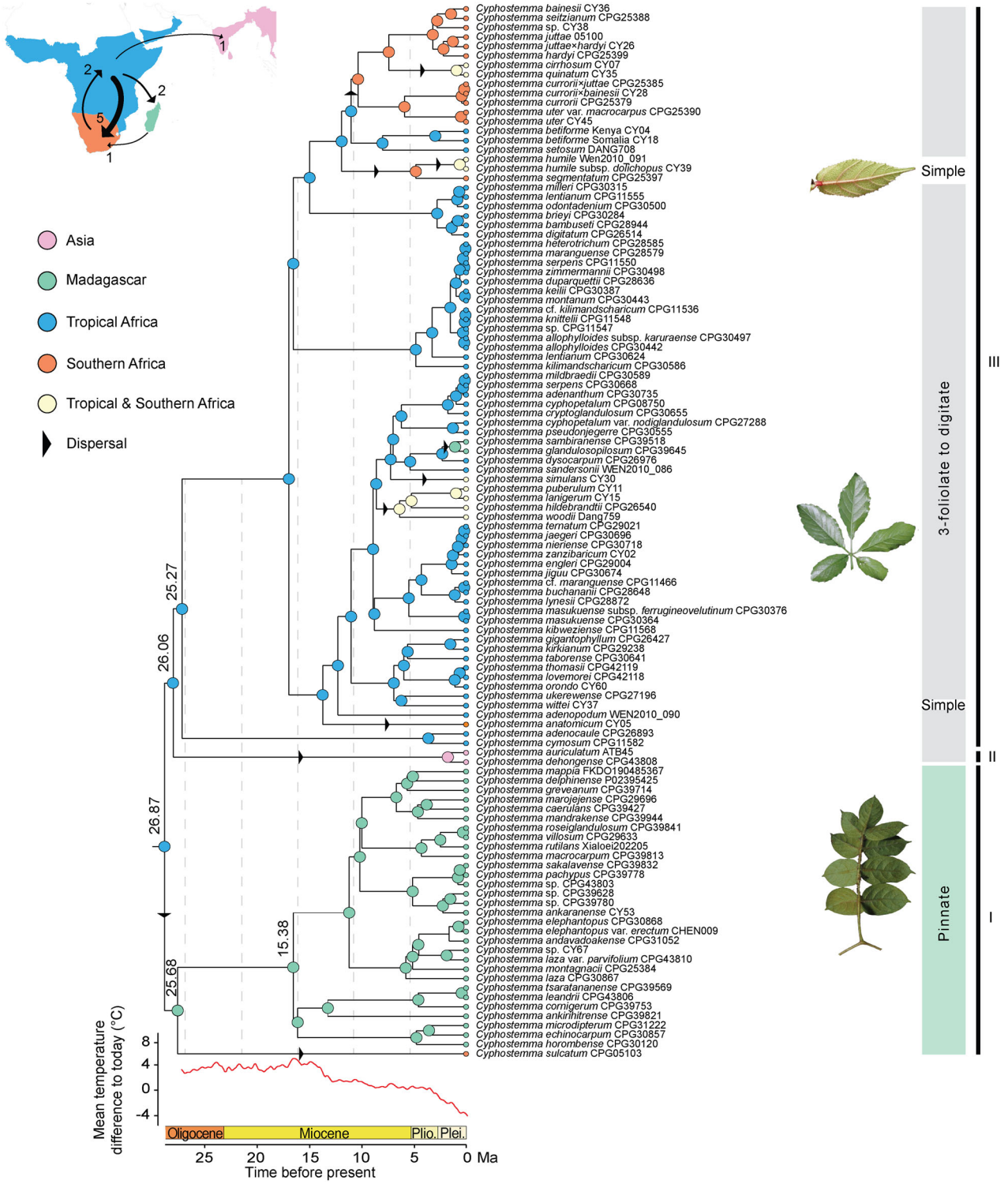

Figure 2. Ancestral area reconstruction of *Cyphostemma* based on the 112-plastome dated phylogeny

A total of 86 accessions were newly sequenced by this study and voucher numbers for sampled individuals are shown after species names. Mean ages for nodes of interest (in millions of years ago, Ma) are displayed nearby, and arrows on the tree indicate the main dispersal events. Colored circles at nodes represent the highest-probability areas, with colors corresponding to biogeographic regions on the map. The red line at the bottom of the figure represents global temperature changes (adapted from Westerhold et al., 2020). Arrows on the map (inset) show the direction of dispersals, with the line thickness proportional to the frequency of dispersal events. Leaf images represent the main types of leaf architecture in *Cyphostemma*, with pinnate leaves in clade I, digitate leaves in clades II, and simple/digitate leaves in clade III.

Africa five times, with two dispersals back to tropical Africa and one migration to Asia. We also identified at least two independent dispersals from tropical Africa to Madagascar. Biogeographic reconstruction based on both the plastid and nuclear datasets yielded broadly similar results, except for species with conflicting phylogenetic positions (Figures 2, S5). As the plastome dataset comprises more taxa, we primarily used the dated tree based on the 112-plastome dataset for subsequent analyses and discussion below.

Diversification and trait evolution in *Cyphostemma*

We identified one major shift in net diversification rate in *Cyphostemma* at ~5 Ma (Figures 3A, S6). Despite an overall constant lineage accumulation through time across the genus, the major clades of *Cyphostemma* exhibit heterogeneous diversification rates (Figures 3A, S6). Clade III (continental Africa) shows an exponential increase in both speciation and net diversification rates under a birth–death model ($r = 0.10$, $\varepsilon = 0.69$, $P < 0.05$; Figure 3B; Tables S2, S3). In contrast, clade I (Madagascar) follows a pure-birth model with linear variation in speciation rate (Table S3) and shows a significantly higher net diversification rate ($r = 0.17$, $P < 0.05$; Table S2). Clade II (Asia) displays the lowest species richness in *Cyphostemma*, with only three extant species currently recognized. This striking asymmetry has also been observed in *Kalanchoe* (Crassulaceae), which has over 150 species in continental Africa and Madagascar but fewer than five in Asia (Rodewald et al., 2025).

We conducted ancestral state reconstructions and trait-dependent diversification analysis for eight morphological traits, comprising succulence, tendrils, leaf habit, tuberous roots, leaf architecture, trichomes, life form, and stem base (Figures S7–S11). While succulence, tendrils, and leaf architecture were previously analyzed in studies with limited taxon sampling and molecular data (Hearn et al., 2018; Rabarijaona et al., 2023; You et al., 2024), our phylogeny, based on broader taxon sampling and high-resolution phylogenomic data, provides new insights into trait evolution in *Cyphostemma*. Four traits (i.e., succulence, tendrils, leaf architecture, and life form) are evolutionarily conserved, showing strong phylogenetic signals (Pagel's $\lambda \geq 0.85$, $P < 0.0001$; Table S4). The most likely ancestral states for these four traits are non-succulent, the presence of tendrils, 3-foliolate to digitate leaf architecture, and a herbaceous life form (Figures S8–S11). Reconstruction of aridity levels indicates multiple transitions from seasonally dry to semi-arid and arid areas over the last 15 Ma (Figure 4F), consistent with repeated colonization of rocky outcrops and the emergence of succulence in both continental Africa and Madagascar (Figures 4, S8 and S12). The best-fitting models for traits analyzed in Binary State Speciation Extinction (BiSSE) and Multi-State Speciation and Extinction (MuSSE) are provided in Tables S5 and S6.

Genome size variation and chromosome number in *Cyphostemma*

We herein report novel genome size data for 72 species and chromosome numbers for 20 species of *Cyphostemma*, and genome size data for 24 species from other lineages of Vitaceae (Figures S13, S14; Tables S7, S8). Flow cytometry analysis generated histograms with a coefficient of variance (CV) < 10% for most of the measurements, using six different internal standards as references (Table S9). We found that the majority of *Cyphostemma* species (88%) investigated had genomes smaller than 2.5 pg (mean = 2.55 pg/1C; *SD* = 1.59, modal = 1.79 pg/1C) (Figure 5A). A clear phylogenetic pattern was observed among arid-adapted species: those in clade I exhibited large genomes (4.20–8.36 pg/1C), whereas most species in clade III (16 out of 21) possessed smaller genomes (1.54–1.86 pg/1C). Notable exceptions within clade III included *C. humile*, *C. humile* subsp. *dolichopus*, and *C. segmentatum*, which are restricted to the southern African carbonate rock habitats and displayed large genomes (3.0–3.25 pg/1C) (Figure 4A, B). The correlation between specific habitat types and larger genome size (Figure 5B) suggests a potential adaptive trajectory distinct from the general trend toward smaller genomes in arid-adapted species. Intriguingly, flow histograms in some succulent diploids exhibited additional peaks (Figure S13), likely indicating the presence of endopolyploid cells.

We inferred a base chromosome number of 11 for *Cyphostemma*, with $x = 10$ occurring occasionally (Figure S15). Diploid species (e.g., *C. leandrii* Desc., *C. dehongense*, and *C. juttae* (Dinter & Gilg) Desc.), with predicted chromosome numbers of $2n = 2x = 22$ (20), had an average genome size of 1.83 ± 0.5 pg. This was significantly smaller than the average genome size of tetraploid ($2n = 4x = 44$; 4.96 ± 2.07 pg) and hexaploid species ($2n = 6x = 66$; 6.17 ± 0.2 pg) (Figure S15). Although sampling limitations prevented a definitive assessment of ploidy frequency across the genus, our correlation analysis revealed a strong positive relationship between genome size and chromosome number ($R^2 = 0.75$, $P = 1.38 \times 10^{-10}$; Figure S16).

Our statistical analyses revealed significant variation in genome size within *Cyphostemma* across aridity levels, habitat types, and succulent states (Figures 5, S17, and S18). Specifically, we found that succulent species in semi-arid to arid regions (aridity index, AI < 0.5) had larger genomes compared to their non-succulent relatives in seasonally dry (0.5 < AI < 0.65) and humid regions (AI > 0.65) (Figure 5A). This pattern aligns with their predominant distribution across rocky outcrops, savannas, and forests (Figure 5B). Although species from seasonally dry regions tended to have smaller genomes than those from humid regions, this difference was not statistically significant. These differences remained robust when independently analyzing genome size data generated using flow cytometry (Figure S17).

Ancestral state reconstruction based on both flow cytometry and simulated genome size data (see Materials and methods) revealed a pronounced genome size expansion in the Malagasy clade I, contrasting with the more conserved genome size evolution observed in Asian and continental African clades (Figure 4A). This pattern remained robust when using exclusively flow cytometry data with internal standardization (Figure S18; Table S7). Precipitation of the driest (Bio17) and coldest (Bio19) quarters was identified as

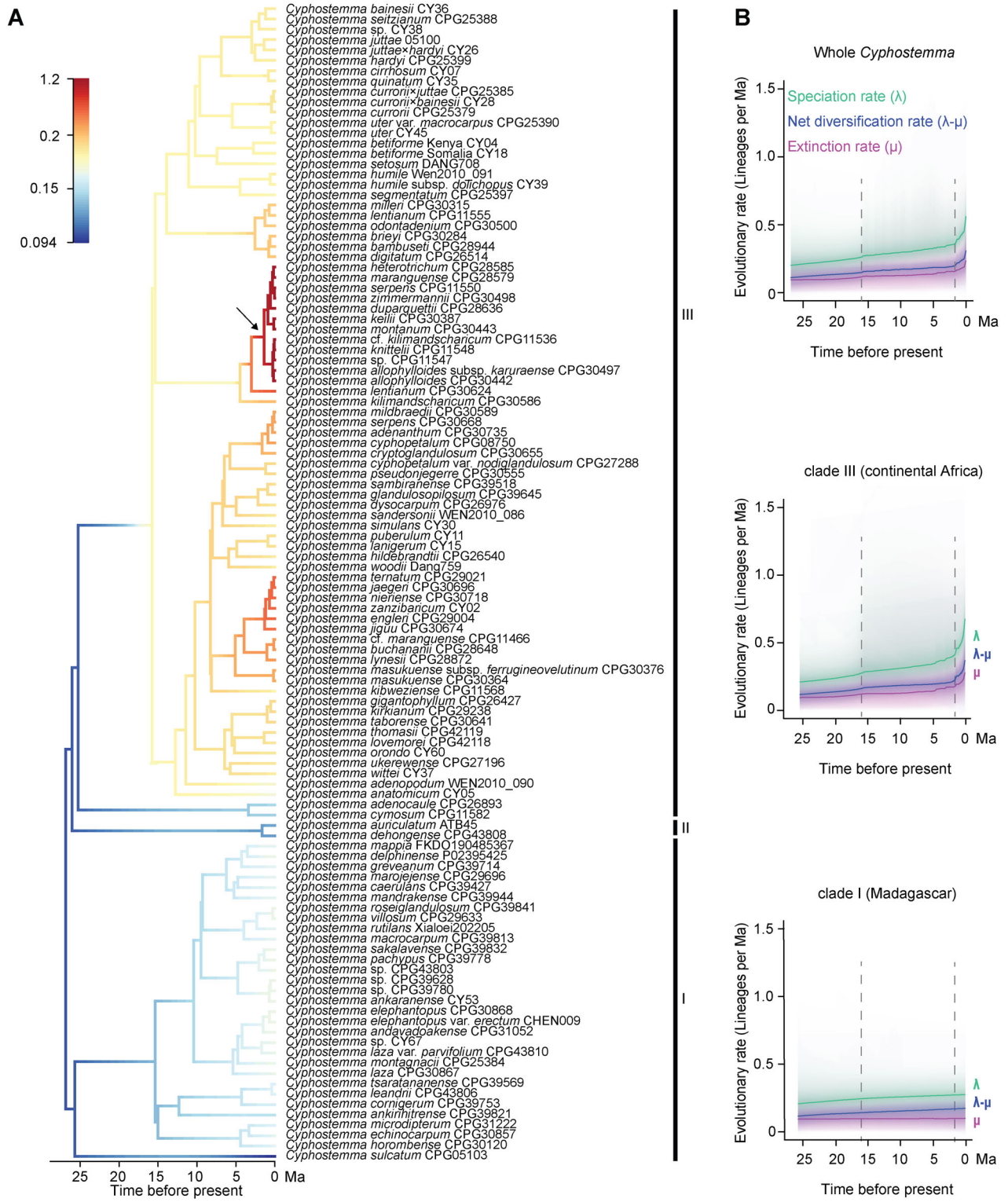

Figure 3. Diversification dynamics in *Cyphostemma*

(A) Phylorate plot from Bayesian Analysis of Macro-evolutionary Mixtures (BAMM) illustrating diversification rate heterogeneity within *Cyphostemma*. The arrow indicates the single significantly supported diversification rate shift identified from the analysis of all *Cyphostemma* species. **(B)** Rate-through time (RTT) plots showing net diversification, speciation, and extinction rates for all *Cyphostemma* species analyzed, the continental African lineage (clade III), and the Madagascar lineage (clade I), with the shaded areas denoting 90% Bayesian credibility intervals. Vertical dashed lines in the plots denote major transitions in the evolutionary rate identified from the analysis of all *Cyphostemma* species.

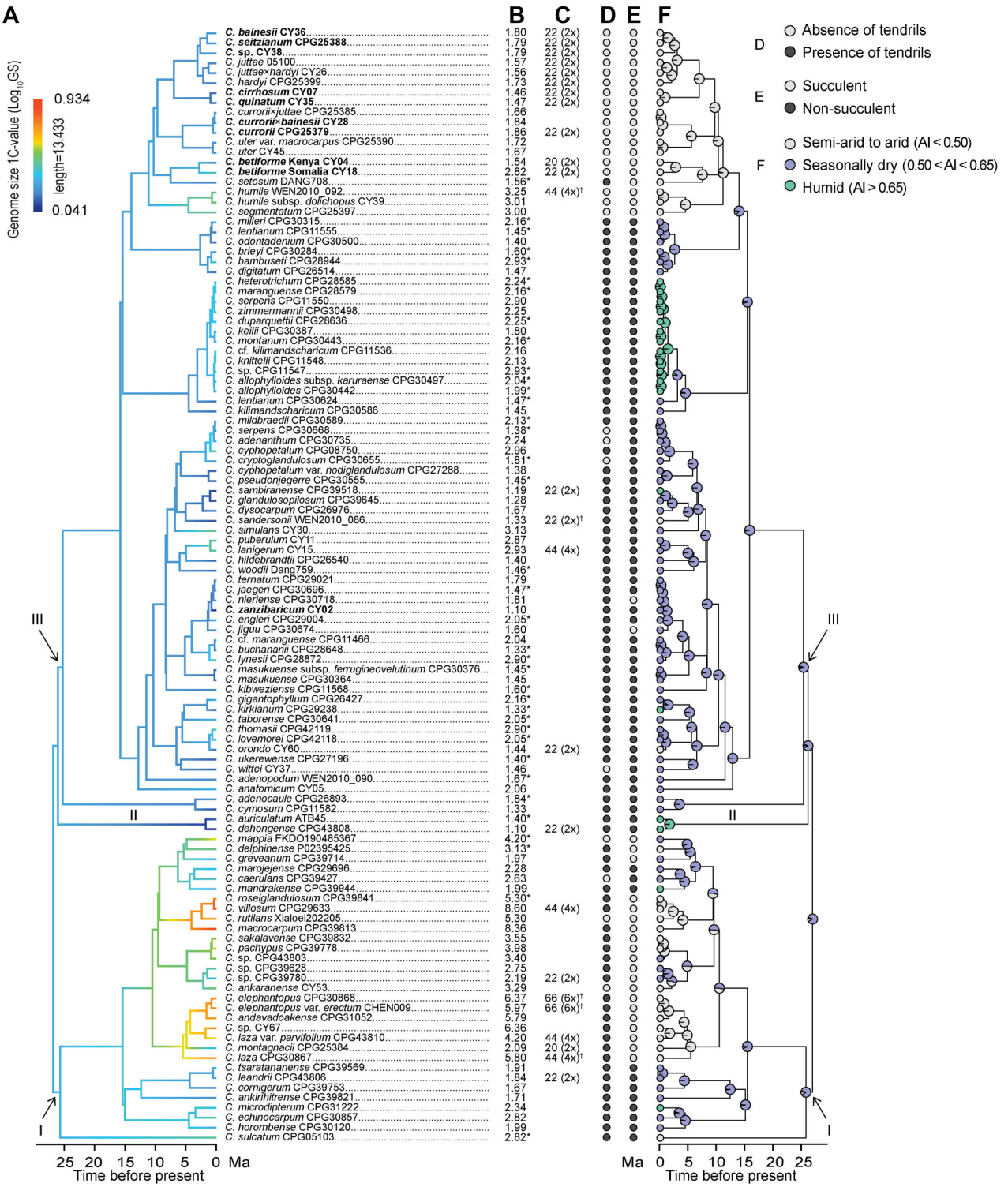

Figure 4. Evolution of genome size and related traits in *Cyphostemma*

(A) Ancestral state reconstruction of genome size based on the 112-plastome phylogeny. Genome size values were Log_{10}-transformed to improve visualization. Voucher numbers for sampled individuals are shown after species names. **(B–C)** Genome size (GS) values for 112 taxa, with 74 measured using flow cytometry (presence of endopolyploid cells highlighted in bold) and 38 marked with "*" corresponding to genome sizes imputed using multivariate imputation by chained equations (MICE) approaches with random forest incorporating morphological, ecological, and bioclimatic variables **(B)**, and chromosome number (ploidy level) for 25 taxa, with 20 taxa measured in this study and five marked with a superscript "†" taken from the literature **(C)**. **(D–F)** Ancestral state reconstructions for traits, including tendrils **(D)**, succulence **(E)**, and aridity level **(F)**.

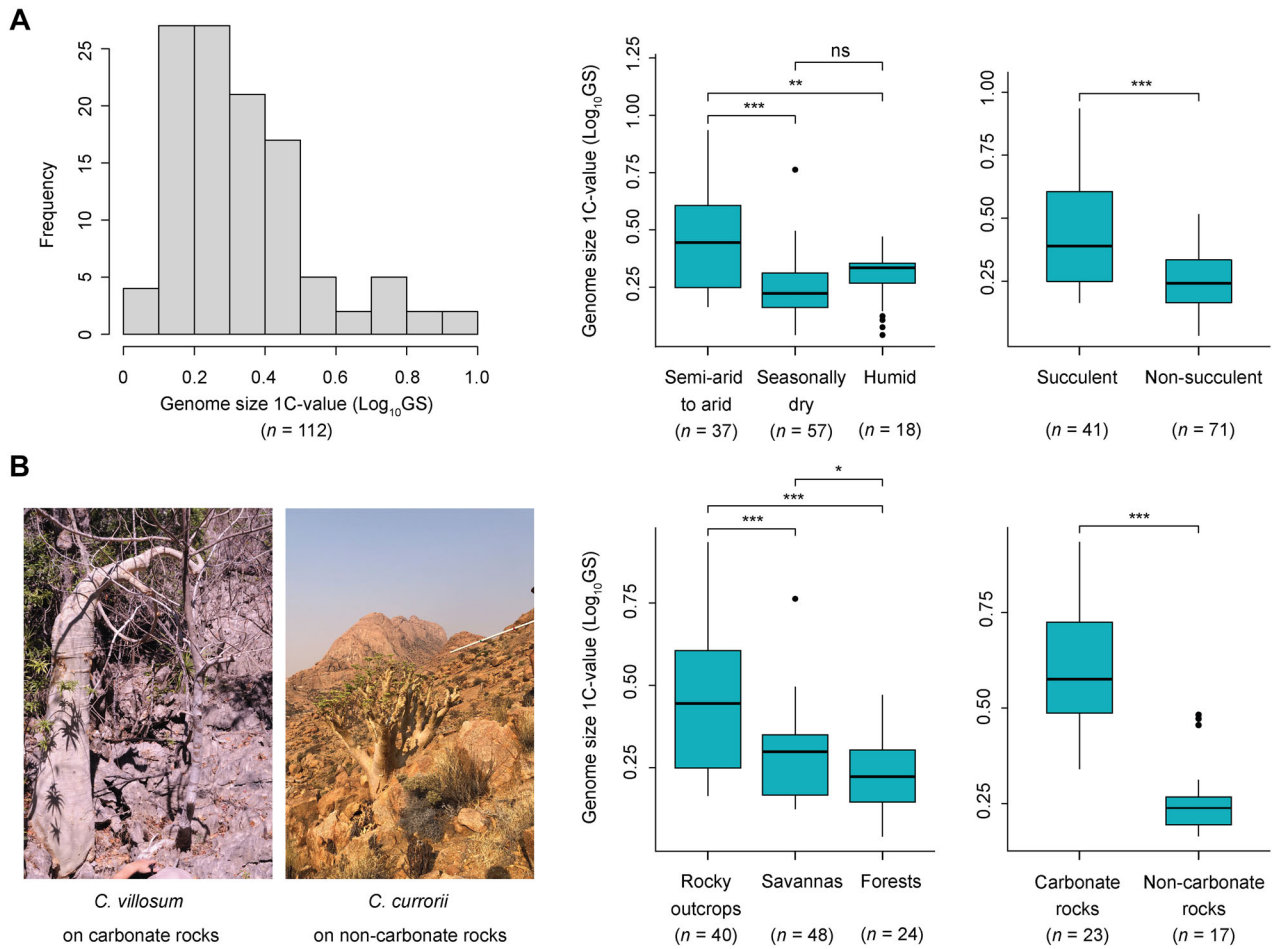

Figure 5. Distribution frequency of genome size and its variation across aridity levels, succulent states, and habitats

(A) Histogram and boxplots showing genome size distribution and variation across aridity levels and succulent states within *Cyphostemma* ($n = 112$). **(B)** Genome size variation across major habitats of *Cyphostemma*, further dividing rocky outcrops into carbonate and non-carbonate rocks, with photos showing *C. villosum* (8.60 pg/1C) on limestone (carbonate) outcrops in Madagascar (Photo credit: Bing Liu) and *C. currorii* (1.86 pg/1C) on non-carbonate rocks in continental Africa (Photo credit: Kay Murray). Genome size values were Log_{10}-transformed to improve visualization. $^{*}P < 0.05$, $^{**}P < 0.01$, and $^{***}P < 0.001$ (ns, non-significant).

the strongest predictor of genome size variation in *Cyphostemma* (Figure S19; Table S10). It was also notable that larger genomes were associated with higher net diversification rates (Figure S20), suggesting a potential role of genome size expansion in the rapid diversification of *Cyphostemma*. These findings represent the first evidence linking genome size dynamics to both environmental adaptation and diversification within *Cyphostemma*.

Genome size variation across eudicots

We assembled a eudicot phylogeny comprising 5,713 species from 1,270 genera and 167 families with available genome size data, using the V.PhyloMaker package (Jin and Qian, 2019) with the GBOTB.extended backbone. We found that 82% of the sampled eudicot species (4,719 species) had small genomes (< 3.5 pg/1C), whereas only ~16% (909 species) and 2% (92 species) exhibited medium (3.5 < GS < 14 pg/1C) and large genomes, respectively (> 14 pg/1C) (Table S11), based on the classification of Leitch et al. (1998). We detected a strong and significant phylogenetic signal for genome size (Pagel's $\lambda = 0.92$, $P = 0.001$) and succulence ($\lambda = 0.77$, $P = 0.001$) (Table S12), indicating that closely related species tend to share these traits. In contrast, aridity level was more evolutionarily labile ($\lambda = 0.57$, $K = 0$, $P > 0.001$) (Table S12), consistent with repeated independent adaptations to arid environments. Moreover, our trait evolution analysis showed that large genomes were highly structured, clustering non-randomly in specific lineages, such as Asterales, Malpighiales, and Santalales (Figure 6).

Our statistical analyses indicated that temperate species ($n = 3,051$) possess significantly larger and more variable genome sizes than those from tropical and subtropical regions ($n = 2,662$) (Figure S21A, B). Furthermore, species from semi-arid to arid regions ($n = 242$) exhibited significantly larger genomes compared to those in seasonally dry ($n = 671$) and humid regions ($n = 4,800$), and succulent eudicots ($n = 149$) had significantly larger genomes than non-succulent species ($n = 5,564$) (Figure 6C). These trends were not significant in temperate regions but were particularly pronounced in tropical

and subtropical regions (Figure S22B). Genome size also varied with life history strategy, as parasitic species ($n = 106$) exhibited significantly larger genomes than their non-parasitic relatives ($n = 5,607$) (Figure S21C, D). This aligns with previous findings that shifts to a parasitic lifestyle are often associated with a massive proliferation of specific repetitive elements, as reported in the holoparasitic Hydnoraceae (Kim et al., 2025).

DISCUSSION

Historical biogeography and diversification dynamics of *Cyphostemma*

Our study establishes the most comprehensive phylogenetic framework for *Cyphostemma* to date, integrating 112 plastomes and nuclear sequence data with expanded taxon sampling across continental Africa and Madagascar. These robust datasets resolve long-standing uncertainties in relationships among the three major clades of the genus and clarify the phylogenetic positions of several previously unresolved taxa (Hearn et al., 2018; Rabarijaona et al., 2023). Notably, the newly included southern African species, *C. sulcatum*, groups within a pinnate-leaf clade (clade I) composed predominantly of Malagasy species, highlighting the evolutionary conservatism of leaf architecture in the genus (Figures 2, S2). This highly resolved phylogeny provides a solid foundation for undertaking biogeographical and diversification analyses, as well as shedding new insights on the patterns of genome size evolution and evaluating its adaptive significance in *Cyphostemma*.

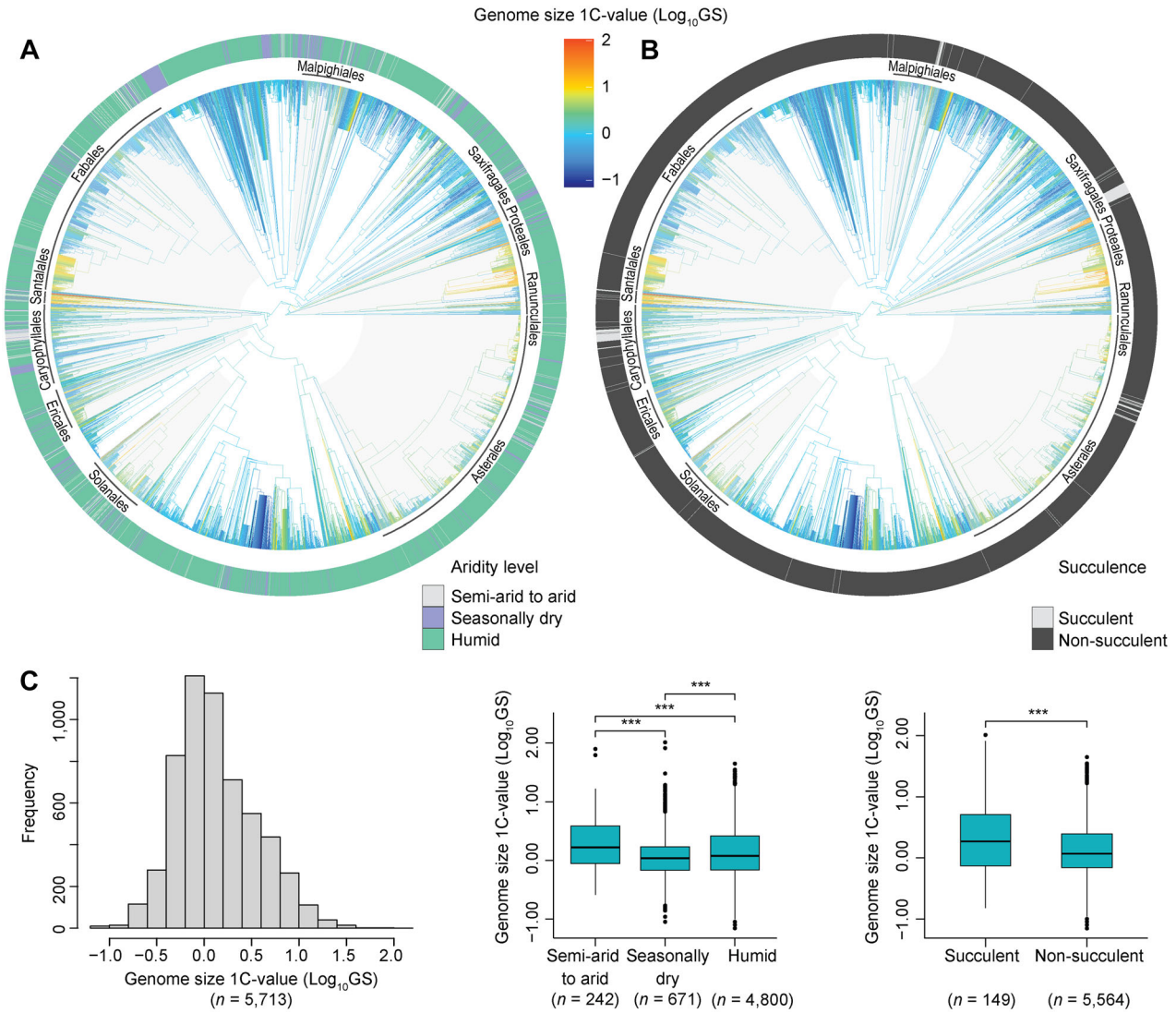

Figure 6. Genome size variation within eudicots in relation to aridity and succulence

(A–B) Evolution of genome size across 5,713 eudicot species within a phylogenetic framework, with the top 10 orders possessing the largest genomes (i.e., > 14 pg/1C) labeled. Aridity levels **(A)** and succulence states **(B)** are mapped onto the phylogeny as colored rings. **(C)** Histograms and boxplots showing genome size distribution and variation across aridity levels and succulence states. Genome size values were Log_{10}-transformed to improve visualization. ***$P < 0.001$ (ns, non-significant).

While previous studies proposed hypotheses regarding the African origin of *Cyphostemma* (Hearn et al., 2018; Rabarijaona et al., 2023; You et al., 2024), due to limited taxon sampling (e.g., a focus on Malagasy species in Rabarijaona et al., 2023) and restricted molecular datasets (e.g., 5cp + 1nu loci in Hearn et al., 2018; CDS + 11cp dataset in You et al., 2024), key questions concerning the directionality of dispersal events remained unresolved. Our biogeographic reconstruction strongly supports a tropical African origin of the genus, followed by repeated back-dispersals from southern Africa (Figures 2, S5). We identified at least two independent dispersals from tropical Africa to Madagascar, consistent with earlier findings on Malagasy *Cyphostemma* diversification (Rabarijaona et al., 2023). The first dispersal occurred in the Oligocene, giving rise to pinnate-leaved species in clade I. Within this clade, our analyses indicate Madagascar as the most probable ancestral area for the pinnate-leaved species (*C. sulcatum*) currently distributed in southern Africa. The second dispersal took place in the Pleistocene within clade III, resulting in two digitate-leaved species in Madagascar (i.e., *C. sambiranense* and *C. glandulosopilosum*). The crown age of *Cyphostemma* (Oligocene/Eocene; node 2 in Figures S3, S4) is much younger than the separation of continental Africa and Madagascar ~121 million years ago (Ma) in the Early Cretaceous (Rabinowitz et al., 1983). This temporal discrepancy strongly supports long-distance dispersal, rather than vicariance, as the mechanism for its current disjunct distribution. Such dispersal events may have been mediated by birds or fruit bats that feed on the colorful, fleshy fruits of *Cyphostemma* (Flörchinger et al., 2010).

Although *Cyphostemma* originated in the Oligocene or late Eocene, its modern diversity primarily stems from a rapid radiation since the late Miocene (Figure 3). This diversification coincided with periods of tectonic uplift and declining atmospheric CO_2, which led to increased aridification and geological ecosystem shifts across Africa (Cerling et al., 1997; Wichura et al., 2010; Pokorny et al., 2015). In continental Africa, the fragmentation of mesic forests created some isolated and unique ecosystems, including the Afromontane forests (Couvreur et al., 2021) and coastal scarp forests (Mucina et al., 2021). Simultaneously, in Madagascar, multiple savanna formations emerged due to interactions among regional climates, fire regimes, and soil heterogeneity (Yoder and Nowak, 2006; Buerki et al., 2013). Together, these environmental shifts provided ecological opportunities for *Cyphostemma* to diversify into newly available niches and to develop specialized local adaptations. Our finding of multiple independent origins of succulence in *Cyphostemma* starting in the late Miocene underscores its repeated and successful adaptation to increasing aridity. This pattern is consistent with other arid-adapted lineages that also radiated with the expansion of global aridification, such as the plants of the Greater Cape region in southern Africa (~17.5 Ma; Verboom et al., 2009) and *Agave* L. from Mexico (~10 Ma; Good-Avila et al., 2006).

Notably, we also identified a major shift in the net diversification rate in *Cyphostemma* at ~5 Ma (Figures 3A, S6), corresponding to transitions from seasonally dry to humid habitats in continental Africa (Figure S7C, D). Our habitat reconstruction revealed repeated shifts between savanna and forest (Figures S7, S8), although most extant species now occur in tropical savannas, reflecting the continued expansion of aridification in Africa since the late Miocene (Chazot et al., 2021). The formation of volcanic mountains during the Plio–Pleistocene eastern Africa uplift may have further promoted this recent rapid diversification by creating new humid habitats (Sepulchre et al., 2006; Chazot et al., 2021; Couvreur et al., 2021). In contrast, the higher net diversification rate and lower extinction rate observed in Madagascar (Figure 3) may be associated with its colonization via long-distance dispersal (Jønsson et al., 2012). Following colonization, speciation rates in early Malagasy lineages gradually increased, a pattern consistent with adaptive radiation into novel environments (Losos and Mahler, 2010). This phenomenon is not unique to *Cyphostemma,* as multiple plant lineages have been shown to undergo spectacular radiations after colonizing Madagascar. Well-documented examples include *Psychotria* (> 160 endemic species; Razafimandimbison et al., 2014, 2017) and *Euphorbia* (> 140 endemic species; Evans et al., 2014). A further notable case is the endemic family Sarcolaenaceae (comprising 10 genera and > 70 species), which likely diverged from a now-extinct African ancestor (Nilsson et al., 1996).

Aridification-linked genome size expansion

Our newly generated genome size data for 72 *Cyphostemma* species has considerably expanded the range of genome sizes known in the genus from 2.44-fold (Chu et al., 2018) to 7.8-fold (1.10 pg/1C in *C. dehongense* to 8.60 pg in *C. villosum* Rabarij. & L.M.Lu) (Figure 5; Table S7). The addition of genome size data for 24 species from other lineages of Vitaceae has also extended the range for the family as a whole, from 10.8- to 28-fold (0.31 pg/1C in *Vitis vulpina* to 8.60 pg in *C. villosum*) (Tables S7, S8). A significant positive correlation between genome size and chromosome number (Figure S16) suggests that recent polyploidization is likely the main underlying cause driving genome expansion in *Cyphostemma*, although the origin of these polyploidization events requires further investigation. Nevertheless, substantial genome size variation among species with the same ploidy level (Figure 5) suggests that proliferation of repetitive DNA elements, particularly retrotransposons, has also played a role in generating genome size diversity.

Our statistical analyses reveal significant genome size variation in *Cyphostemma* between aridity levels, succulence traits, and habitat types (Figures 5, S17 and S18). Specifically, we find that succulent species from semi-arid to arid regions exhibit larger genomes compared to their relatives from seasonally dry or humid habitats (Figure 5A). Our comparative study across eudicots reveals broader, previously unexplored trends linking larger genomes with succulence and arid habitats (Figure 6). This pattern is particularly significant in species from tropical and subtropical regions (Figure S22B). These findings suggest that the persistent

stress in semi-arid to arid environments (e.g., drought, high temperature, and elevated UV-B), which can trigger repetitive DNA amplification and polyploidization leading to genome size expansion, may be compatible with the emergence of succulent traits. Such expansion could have provided opportunities for the evolution of more complex genetic toolkits and trait innovation, enabling these plants to thrive in extreme conditions (Nevo, 2001; Ohri, 2005; Griffiths and Males, 2017; Li et al., 2024; Omollo et al., 2024).

Genome size expansion may also have been beneficial in succulent plants, with the larger cell sizes providing increased water storage capacity (Ohri, 2005; Pacey et al., 2022). If accompanied by a reduction in stomatal number, this could have reduced stomatal conductance compared to species with smaller genome sizes, leading to enhanced water-use efficiency (Hetherington and Woodward, 2003). This is consistent with the trend in Crassulacean acid metabolism (CAM) plants, an adaptation for minimizing water loss through transpiration, which typically have larger genomes than related C_3 species (Roddy et al., 2020; Sage et al., 2023). The presence of CAM photosynthesis in some succulent *Cyphostemma* (Virzo De Santo et al., 1983; Gilman et al., 2023) suggests a potential link between genome size and this water-saving strategy, but more data are needed to confirm its functional significance and evolutionary role.

Divergent adaptive strategies in continental Africa and Madagascar

We detect distinct geographic patterning in genome size evolution within *Cyphostemma* (Figures 4A, S18). The genome size expansion in Madagascar mostly occurs in succulent, polyploid species, while the succulent species from continental Africa are mostly diploids with smaller genome sizes (Figure 4A–C). Although these succulent plants all occur in semi-arid to arid environments and grow in similar habitats in both continental Africa and Madagascar (Figures 4D–F, S8A, and S12), the two lineages seem to follow distinct patterns of genome size evolution in their respective geographic locations. Southern Africa has been categorized as an old, climatically buffered infertile landscape (OCBIL; Hopper et al., 2021), with most species resolved in phylogenetic positions that are sister to the main lineages and on long branches, such as *C. sulcatum* and *C. anatomicum* (Figure S5). These species might have evolved distinct adaptive strategies to thrive in these harsh environments (Beatriz et al., 2021). Madagascar possesses young geological landscapes, with more volcanic activity and diverse ecosystems that have contributed to richer and more fertile soils, while southern Africa presents older landscapes dominated by savanna and grassland vegetation, which may have led to a lower nutrient content in the soil (Antonelli et al., 2022). Such observations are relevant, as an increasing number of studies are showing that plant communities growing on sites with low levels of nutrients, particularly nitrogen and phosphorus, are typically characterized by species with smaller genome sizes compared to those found on high-nutrient sites (Kang et al., 2015; Leitch and Leitch, 2022; Morton et al., 2024).

Other studies have reported that at least 5%–10% of plant species exhibit edaphic specialization correlated to underlying bedrock types (Lichter-Marck and Baldwin, 2023; Zhao et al., 2024). Our investigation of *Cyphostemma* on rocky outcrops reveals an intriguing genomic divide between substrates: Species on mineral-rich carbonate rocks have significantly larger genomes than those on non-carbonate substrates (Figure 5B). The divergence is mirrored in their geography and ploidy: Carbonate-associated species are mostly succulent polyploids locally endemic to Madagascar's limestone outcrops (e.g., *C. villosum*, *C. elephantopus* Desc., and *C. laza* Desc.), whereas species on non-carbonate rocks are typically succulent diploids from southern Africa (e.g., *C. bainesii* (Hook.) Desc., *C. seitzianum* (Gilg & M.Brandt) Desc., *C. currorii* (Hook.f.) Desc.). We propose that the stressful, yet stable, low-competition environment of carbonate outcrops might enable the persistence of species with large genomes given their association with traits, such as their increased water storage capacity (e.g., Pacey et al., 2022), which may outweigh some of the disadvantages associated with bigger genomes, such as slower growth, rate of cell production, and longer life cycles (e.g., Bilinski et al., 2018; Guignard et al., 2019).

Polyploidy, which, at least initially, gives rise to larger genomes, may have driven the diversification of the genus in Madagascar (Figure 4A) via facilitating the establishment of species in isolated limestone outcrops, by conferring them with higher genetic diversity and hence potentially greater ecological tolerance (Meudt et al., 2021, Van de Peer et al., 2021). In contrast, diploid species in southern Africa, where genome size appears to be more constrained due to the low nutrient levels, may have taken advantage of endopolyploidy as a mechanism to provide increases in cell size only in the tissues needed for water storage. Such an approach minimizes the added nutrient costs of maintaining large genomes in all cell types, while benefiting from producing large cells where they are needed (De Rocher et al., 1990). Intriguingly, our flow cytometry results show that endopolyploid cells occur mainly in the succulent and diploid species from southern Africa (taxa in bold; Figure 4). Endopolyploidy has also been reported in numerous other succulent plants (e.g., De Rocher et al., 1990; Powell et al., 2020) to cope with low-nutrient soils from non-carbonate rocks. The balance of nutrient availability, particularly nitrogen and phosphorus, may have played a crucial role in shaping plant evolutionary strategies (Guignard et al., 2019; Leitch and Leitch, 2022).

In conclusion, our results provide new insights into the diversification dynamics and genome evolution of *Cyphostemma*, a species-rich genus in sub-Saharan Africa. We identify a significant increase in diversification rates during the Late Miocene/Pliocene (~5 Ma), coinciding with the expansion of aridification and mountain uplift across Africa. This synchrony suggests that these major environmental changes were probably involved in creating ecological

opportunities that shaped the complex evolutionary history of *Cyphostemma*, emphasizing the aridification-linked radiation of this and other African plant lineages. Furthermore, we recognize a strong association between larger genomes and polyploid species that possess succulent traits and occupy limestone habitats in *Cyphostemma*. Our broad analysis across eudicots reveals a previously unexplored macroevolutionary trend: Larger genome sizes are significantly more prevalent among succulent species from arid habitats compared to their non-succulent relatives in more mesic habitats. This pattern is particularly pronounced in tropical and subtropical biomes. In addition, we observe distinct genome size patterns between succulent *Cyphostemma* lineages from continental Africa and Madagascar, suggesting important roles of polyploidization and endopolyploidy associated with the evolution of succulence and aridification adaptation. These processes appear to be facilitated by sufficient nutrient availability from specialized soil and bedrock substrates, enabling plants to overcome nutrient-related physiological constraints imposed by large genomes. This study lays a solid foundation for future investigations into the genomic mechanisms and ecological drivers of genome size expansion in succulents. The findings also highlight the conservation urgency for these spectacular plants in the face of escalating anthropogenic pressures and climate change, especially given the recent findings that herbaceous species with larger genomes are at greater risk of extinction than those with smaller genomes (Soto Gomez et al., 2024).

MATERIALS AND METHODS

Taxon sampling and data processing

We reconstructed phylogenies of *Cyphostemma* using plastome and single-copy nuclear gene sequences. We newly generated complete plastome sequences for 67 species of *Cyphostemma*, including the pinnate-leaved species from southern Africa in particular, and combined them with 45 complete plastome sequences from our previous study (Rabarijaona et al., 2023). This resulted in a comprehensive dataset of 112 *Cyphostemma* species (112-plastome dataset), representing 56% (i.e., 112/200 spp.) of species richness, covering its major taxonomic and geographical diversity. We expanded the data to a 159-plastome dataset by adding 47 other Vitaceae species and two *Leea* D.Royen species as outgroups for divergence time estimation (Table S13).

The sequences were obtained using the Illumina HiSeq platform by Novogene Bioinformatics Technology Co. Ltd. (Beijing, China). We assembled the plastome sequences using GetOrganelle v.1.7.1 (Jin et al., 2020) and annotated them with GeSeq v.1.79 (Tillich et al., 2017) using the plastid genome of *Vitis vinifera* L. (NC007957) as a reference. The boundaries of the large single-copy (LSC), small single-copy (SSC), and inverted-repeat (IR) regions for each sequence were manually adjusted in Geneious v.8.1.9 (Kearse et al., 2012). Each plastome contained approximately 101 coding genes, including four rRNAs, 29 tRNAs, and 120–124 intergenic regions. A total of 79 coding sequences were used for phylogenetic reconstruction, with only the IRb retained, as sequences of the two IR regions were identical.

Nuclear genes were retrieved through the HybPiper pipeline v.1.3.1 (Johnson et al., 2016) to target 229 single-copy orthologs selected by Wen et al. (2013). The filtered reads were first mapped to the target genes using the default aligner BWA (https://github.com/lh3/bwa). SPAdes v.3.12.0 (https://github.com/ablab/spades) was then used to assemble reads into contigs. The assembled contigs were aligned to the reference target sequences using Exonerate (https://github.com/nathanweeks/exonerate). To ensure data quality, potential paralogs identified with the "paralog_investigator" option of HybPiper were removed. The sequences were then aligned and trimmed with MAFFT v.7.450 and trimAl v.1.2 with the option "automated1." We recovered 229 nuclear genes for 80 *Cyphostemma* species and three *Cayratia* outgroup species (83taxa-229nu dataset). Finally, a nuclear time tree was built based on an expanded dataset including 104 Vitaceae species for the same 229 nuclear genes (104taxa-229nu dataset).

Phylogenetic reconstruction and divergence time estimates

Given the frequent occurrence of cytonuclear discordance in Vitaceae (e.g., *Causonis*, Yu et al., 2023b; *Parthenocissus*, Yu et al., 2023a; and *Vitis*, Nie et al., 2023), we compared phylogenetic topologies inferred from the 83-plastome and 83taxa-229nu datasets. Phylogenetic reconstruction for the plastome dataset was conducted using the maximum likelihood (ML) approach in IQ-TREE v.2.1.2 with 1,000 ultrafast bootstrap replicates (Nguyen et al., 2015). The best-fitting nucleotide substitution model (TVM + F + R6) was selected by ModelFinder v.1.6.1. Nodes with bootstrap support (BS) > 95% were considered to be well-supported (Hedges, 1992). For the 83taxa-229nu dataset, single gene trees were first constructed with the GTRCAT model in IQ-TREE. Then a species tree was built using the coalescent approach implemented in ASTRAL v.5.6.3 (Mirarab et al., 2014). Trees were visualized using FigTree v.1.4.4 (http://tree.bio.ed.ac.uk/software/figtree/).

Divergence times were estimated based on both the 159-plastome and the 104taxa-229nu datasets. We constrained the stem age of Vitaceae to 90.7 ± 1.0 million years ago (Ma) with a normal prior distribution using a secondary calibration in Magallón and Castillo (2009) according to previous studies (Lu et al., 2013; You et al., 2024). Since the Cayratieae tribe lacks reliable fossil records, we used *Ampelocissus parvisemina* Chen & Manchester, the confirmed seed fossil of Vitaceae from the late Paleocene of North America (Chen and Manchester, 2007), to constrain the crown age of the *Ampelocissus–Vitis* clade (see stars in Figure S3) following Nie et al. (2023) and Rabarijaona et al. (2025). We applied a lognormal distribution (mean: 58.5 Ma; log (stdev): 0.03; offset: 0 Ma; mean in real space) to encompass the 95% HPD interval of the fossil date (56.8–62.0 Ma).

For the plastome dataset, we performed dating analysis in BEAST v.2.4.8 on the CIPRES portal (Miller et al., 2010) using a Yule speciation tree prior and the GTR + I + G substitution model. We ran the Markov Chain Monte Carlo (MCMC) chain for 250,000,000 generations, with parameters sampled every 10,000 generations. We assessed convergence in Tracer v.1.7.1 (Rambaut et al., 2018), ensuring effective sample sizes (ESS) for all parameters > 200. A chronogram with median node ages and 95% highest posterior density intervals (95% HPDs) was generated in TreeAnnotator v.2.4.8 after discarding the first 25% of trees as burn-in.

For the nuclear dataset, divergence time estimation was carried out using MCMCTree in PAML 4.9j (Yang, 2007), with the following settings: birth–death model, correlated rates, and HKY85 substitution model with alpha = 0.5. We combined the results of two independent MCMC chains with the first 20% of iterations discarded as burn-in, where samples were drawn every 10,000 generations until the ESS was > 200 for all parameters. The final dated trees based on both the 159-plastome and 104taxa-229nu datasets were viewed and edited using FigTree.

Biogeographic reconstruction and diversification analyses

Biogeographic reconstruction for *Cyphostemma* was conducted using the ML method in BioGeoBEARS (Matzke, 2014) implemented in RASP v.4.2 (Yu et al., 2020), with the dated plastid and nuclear phylogenies pruned to retain only *Cyphostemma* species as input trees. We defined four biogeographic areas according to the current distribution of the genus: (A) tropical Africa; (B) southern Africa; (C) Madagascar (including Comoros and Mauritius islands); and (D) Asia. We tested three basic models in BioGeoBEARS (i.e., DEC, DIVALIKE, and BAYAREALIKE), with or without the "jump dispersal" parameter j, which weights founder-event speciation in the evolutionary estimation (Matzke, 2012). The optimal model was selected according to the corrected Akaike information criterion (AICc).

Diversification dynamics of *Cyphostemma* were estimated based on the pruned dated plastid tree. BAMM v.2.5.0 was used to explore the overall diversification dynamics of *Cyphostemma*. Prior values were selected using the "setBAMMpriors" function using the R package "BAMMtools" v.2.5.0 (Rabosky et al., 2014) with a sampling proportion of 0.56. The MCMC was run for 50 million generations, sampling every 1,000 generations. Post-run analyses were performed in BAMMtools, with an initial 10% discarded as burn-in, and the remaining data were assessed for convergence with ESS values > 200. Rate-through-time plots were generated using the "PlotRateThroughTime" function for the entire genus as well as its three major clades.

We detected distinct rate shift configurations with the highest maximum a posteriori (MAP) probability ("the best shift configuration"). We computed the 95% credible rate shift configurations using the Bayes factor criterion, setting nodes as core shifts to 5. Distinct shift configurations and their frequencies were obtained as the posterior probability of each configuration to explain the evolutionary dynamics of diversification in *Cyphostemma*. Models of diversification, including diversification, speciation, and extinction rates, were estimated using MEDUSA (modeling evolutionary diversification using stepwise AIC) in the R package "Geiger" (Pennell et al., 2014). We tested different models and particularly compared the Yule model (Yule, 1925), a pure-birth model in which speciation events are independent of one another with a constant rate over time, with a birth–death model, which is similar to the Yule model, but with a constant extinction rate over time. The best-fitting models of diversification in *Cyphostemma* were selected based on the corrected AICc.

We also used the R package "RPANDA" (Morlon et al., 2016) to further explore the models of diversification among the *Cyphostemma* clades. Four different scenarios with all combinations of constant and variable speciation and extinction rates were used to fit different models of rate variation through time. The best-fitting model was selected using the maximum likelihood method based on the AICc. We generated semi-logarithmic lineage-through-time (LTT) plots from the MCC tree and randomly selected 1,000 posterior trees from the BEAST analysis to visualize the temporal dynamics of diversification in *Cyphostemma* using the R package "ape" v.5.7 (Paradis et al., 2004). We also fitted different models of diversification, speciation, and extinction rates to select the best model for the diversification dynamics of clade I (mainly from Madagascar) and clade III (mainly from continental Africa) of *Cyphostemma*. Clade II (from Asia) was excluded from this comparative analysis because of its low species number.

Trait selection and ancestral state reconstruction

We performed ancestral state reconstruction for eight morphological characters (i.e., succulence, tendrils, leaf habit, tuberous roots, leaf architecture, trichomes, life form, and stem base) and two ecological factors (habitat type and aridity level) to investigate their evolutionary history (Table S14). These traits were selected because previous studies with limited sampling suggested their potential roles in ecological adaptation (e.g., Hearn et al., 2018; Rabarijaona et al., 2023; You et al., 2024). Our comprehensively sampled phylogeny allows us to test these hypotheses explicitly.

The habitat, trait, and distribution data of *Cyphostemma* were collected from herbarium specimens, efloras (http://www.efloras.org/), Plants of the World Online (https://powo.science.kew.org/; accessed in August 2020), Global Biodiversity Information Facility (GBIF, https://www.gbif.org/; accessed in February 2024), and our fieldwork observations. We confirmed species identification by checking available voucher specimens and images (Table S14).

Ancestral state reconstruction was conducted using the "fastAnc" function (fast ML estimation) and visualized on the tree with the "contMap" function, both implemented in the R package "phytools" (Revell, 2012). As fine-scale habitat

variability may influence the occurrence and local adaptation of plant species, we applied a two-step strategy for habitat reconstruction. First, we inferred the ancestral habitat state by coding three states (rainforests, savannas, and rocky outcrops) for species of *Cyphostemma* to determine the potential transition between habitat types. Then, each species was assigned to one of the three broad habitat categories based on the AI: humid ($AI > 0.65$), seasonally dry ($0.50 < AI < 0.65$), and semi-arid to arid ($AI < 0.50$), according to the aridity level of their current geographical occurrences (Peel et al., 2007).

Trait-dependent diversification analyses

To evaluate whether net diversification rates are associated with trait states or habitat shifts, we implemented state-dependent speciation-extinction (SSE) models. Using the R package "diversitree" v.0.9.10 (FitzJohn, 2012), we applied both binary-state (BISSE) and multi-state (MuSSE) analyses. For each character, we fitted five models: (i) a full unconstrained model; (ii) a model with equal extinction rates (μ) across states; (iii) a model with equal speciation rates (λ); (iv) a model with equal transition rates (q); and (v) a model constraining both μ and q. The best-fitting model was selected based on the likelihood ratio tests under a chi-square distribution and AICc (Akaike, 1974).

Genome size measurements using flow cytometry

We measured the genome size (C-value) of 72 species of *Cyphostemma* using flow cytometry, mainly based on six different internal standards as references (Table S9), and included data for two additional species from the literature (Chu et al., 2018). We employed flow cytometry, the most frequently applied method, to estimate the absolute genome size of *Cyphostemma*. We followed the chopping method described by Galbraith et al. (1983). Nuclear suspensions from leaves were prepared with Galbraith-modified buffer (PVPK12-mGB2: 30 mmol L^{-1} sodium citrate, 45 mmol L^{-1} $MgCl_2$, 20 mmol L^{-1} MOPS, 20 mmol L^{-1} NaCl, 20 mmol L^{-1} EDTA Na_2H_20, 0.1% (w/v) Triton X-100, 0.5% (v/v) Tween-20, 10 μL mL^{-1} β-mercaptoethanol, 1% PVP K12, pH 7.0) and stained with 100 μg mL^{-1} propidium iodide (PI-Absolute) and 0.5 μg mL^{-1} RNase (Loureiro et al., 2006, Doležel et al., 2007). Stained nuclei were analyzed using a BD LSRFortessa™ Cell Analyzer.

We established two protocols for genome size measurement using two types of standardization procedures. For each of the two methods, we first ran the target sample alone and adjusted the voltage according to the relative fluorescence of the sample (Sharrow, 2002), where a lower voltage corresponds to a larger genome size. Then, we selected the appropriate calibration reference standard to enable us to convert the relative fluorescence of the target species into an absolute genome size (see more details of genome size measurement using flow cytometry in Supplementary methods).

Genome size simulation for missing data

Researchers usually handle missing data by omitting the ones for which some observations are not available, but this can lead to a huge reduction in the data size. In this study, we acquired flow cytometry data for 72 species and genome size records for two additional species from the literature (Chu et al., 2018). As genome size data for 38 of the 112 species (i.e., 34%) in our phylogenetic tree were missing, we addressed this gap in genome size data using the multivariate imputation by chained equations (MICE) method to simulate input data via a random forest algorithm (Shah et al., 2014).

We first tested the correlation between genome size and all eight morphological traits, as well as habitat types and aridity level, which significantly correlated with genome size variation in *Cyphostemma* with a strong phylogenetic signal ($0.85 < \lambda < 1.0$). Phylogenetic signals were tested using Pagel's λ (Pagel, 1999) and Blomberg's K. (Blomberg et al., 2003). The best-fitting model for trait evolution and its covariance structure were selected from the following models: (i) absence of phylogenetic signal; (ii) neutral Brownian motion; (iii) constrained evolution Ornstein–Uhlenbeck (OU); and (iv) early burst (EB) models; based on AIC in generalized least squares (GLS) methods. Most traits followed an OU process rather than Brownian motion (BM), with the exception of an EB model, which was identified as the best model for life form and leaf architecture (Table S4).

We then performed the phylogenetic generalized least-squares method (PGLS) in the R package "caper" (Orme et al., 2013) to assess whether genome size variation within *Cyphostemma* was correlated with environmental factors. Median values of the 19 bioclimatic variables were obtained from the Chelsa climate database (https://chelsa-climate.org/bioclim/; accessed in September 2022). We also included three variables: AI, potential evapotranspiration (PET) from the Global Aridity Index and Potential Evapotranspiration Climate database (https://figshare.com/articles/dataset/Global_Aridity_Index_and_Potential_Evapotranspiration_ET0_Climate_Database_v2/7504448/3; accessed in September 2022), and elevation. We simulated the genome size values for missing data using bioclimatic variables, morphological traits, and habitat type as predictors. These predictors were chosen from the 22 bioclimatic variables (Table S10) based on their significant influence on genome size variation in *Cyphostemma* (significant at $P < 0.05$), and phylogenetic signal for morphological traits and habitat type ($\lambda > 0.85$). The correlations between environmental factors were first calculated using the pairwise Pearson's test to exclude extremely collinear variables and retained only 10 bioclimatic variables. We also applied an alternative approach using PGLS to select the most significant variables among 22 bioclimatic variables since many *Cyphostemma* species are restricted to specific habitats.

Four morphological traits (succulence, life form, tendrils, and leaf architecture), three habitat types (rainforests, savannas, and rocky outcrops), and nine bioclimatic variables

from Chelsa dataset (Bio02: Temperature Mean Diurnal Range, Bio07: Temperature Annual Range, Bio12: Annual Precipitation, Bio13: Precipitation of Wettest Month, Bio14: Precipitation of Driest Month, Bio15: Precipitation Seasonality, Bio16: Precipitation of Wettest Quarter, Bio17: Precipitation of Driest Quarter, Bio19: Precipitation of Coldest Quarter) plus AI) were finally selected as the predictor variables for imputing missing genome size data. For the total sampling of 112 taxa included in the phylogenetic tree, we compiled these variables and used them as predictor variables in the MICE methods (Burgette and Reiter, 2010). To test the accuracy of the methods, we also simulated the genome size for 74 taxa with known values and calculated the variances and standard deviations (Tables S7, S15).

Chromosome counts from mitotic and meiotic cells

Chromosome numbers for 20 *Cyphostemma* species were counted, 17 of which were newly reported, while three confirmed the counts reported in previous studies (Lavie, 1979; Chu et al., 2018). Mitotic chromosome counts were performed on the meristematic tissue from root tips with actively dividing cells, using a conventional squash method following Zhang (1998), with slight adjustments to the timing and staining procedures. For counts based on meiotic material, the procedures outlined in Sinha et al. (2016) and Hiremath and Chinnappa (2015) were used with modifications in the timing of floral bud collection and the duration of exposure to Carnoy's fixative solution. The slides for chromosome counting were observed under a light microscope (Upright Microscopes Leica DM6) with an integrated Leica Application Suite (LAS) software platform in the State Key Laboratory of Systematic and Evolutionary Botany, Institute of Botany, Chinese Academy of Sciences (Beijing, China). The relationship between genome size and chromosome number was evaluated using a PGLS regression model, implemented with the "gls" function in the R package "nlme" (Pinheiro et al., 2021).

Genome size evolution in *Cyphostemma*

We reconstructed the evolutionary history of genome size using a maximum likelihood approach with the "fastAnc" function and visualized the ancestral states on the phylogeny using the "contMap" function, both implemented in the R package "phytools." To evaluate the impact of ecology on genome size, we compared genome size variation across aridity levels and succulent states using the "*t*-test" function from the R package "rstatix" (Kassambara, 2022). We further tested the influence of bedrock substrate by dividing the rocky habitats of *Cyphostemma* into carbonate rocks and non-carbonate rocks (Flügel, 2010). The results were visualized using the "ggboxplot" function in the R package "ggpubr."

We also conducted trait-dependent diversification analysis for small and large genomes in *Cyphostemma*. Following the angiosperm-wide framework of Leitch et al. (1998), "small" genomes were defined as < 3.5 pg/1C and "large" genomes as > 14 pg/1C. For our *Cyphostemma*-specific analysis, we adjusted these thresholds based on the mean genome size (2.5 pg/1C) of our dataset, defining small genomes as ≤ 2.5 pg/1C and large genomes as > 2.5 pg/1C. We then applied the BiSSE model to compare diversification rates between these two states.

Genome size evolution across eudicots

To explore the broader implications of our findings, we expanded our analyses to examine genome size evolution across angiosperms. We focused on testing its correlation with aridity and succulence. Since genome size is unevenly distributed between the major groups of angiosperms (Henniges et al., 2023), with the monocots possessing the most diverse genome sizes (mean = 9.58 pg, $SD = 12.55$), which are significantly larger on average than those of eudicots (mean = 2.50 pg; $SD = 3.93$). Very large genomes ($1C \geq 50$ pg) are most common in monocots, though some occur in the eudicot order Santalales (Pellicer and Leitch, 2020).

We downloaded genome size data for 6,614 eudicot species from the Plant DNA C-values database (https://cvalues.science.kew.org/, accessed in February 2024). To enable phylogenetic comparative analysis, we constructed a comprehensive phylogeny of these species using the R package "V.PhyloMaker" (Jin and Qian, 2019) with the backbone tree "GBOTB.extended" and scenarios = "S1." We first filtered the dataset by removing duplicates and retaining the most recent GS measurements. Taxonomic mismatches between the phylogeny and species list from the Plant DNA C-values database were manually curated to follow the Plant DNA C-values database. Species with ambiguous or missing data for succulence or aridity were excluded, retaining a final dataset of 5,713 eudicot species. The complete species list is provided in Table S11, and the phylogeny is available at ScienceDatabase (https://doi.org/10.57760/sciencedb.28584).

Trait data for biome, succulence, and parasitism were collected from Plants of the World Online (accessed in July 2025). To determine aridity level, we extracted data from the Chelsa climate database (https://chelsa-climate.org/bioclim/; accessed in July 2025) using the most frequent occurrence points for each species. Occurrence data were obtained from the GBIF using the R package "rgbif" (Chamberlain et al., 2022) and rigorously filtered to remove outliers and unreliable records (Table S11). Given the distribution of our focus taxa *Cyphostemma* in sub-Saharan Africa, we specifically compared genome size variation between temperate versus tropical and subtropical eudicots across aridity levels and succulent states. We also quantified the relationship between genome size variation and parasitism states to test for alternative evolutionary drivers. For each trait, we assessed phylogenetic signal (Pagel's λ and Blomberg's K) to evaluate evolutionary patterns and their correlation with genome size variation.

Data availability statement

The newly generated short reads used for phylogenetic reconstruction have been deposited in the NCBI Sequence Read Archive (BioProject PRJNA1320927). Vouchers for all sampled Vitaceae species are provided in Table S13. Genome size, chromosome number, morphological traits, habitat types, aridity level, and bioclimatic variables for *Cyphostemma* species are provided in Table S14. Genome size, distribution, climate, aridity level, and succulent states for 5,713 eudicots are provided in Table S11.

ACKNOWLEDGEMENTS

We thank Jian-Fei Ye, Xiao-Lei Lin, Cheng-Xin Fu, Pan Li, Run-Xian Yu, Quan Xing, and Anna Trias-Blasi for field assistance and/or sample collection. We are grateful to our collaborators from the Mention Biologie et Ecologie Végétales (MBEV)-Université d'Antananarivo, Madagascar, the Ministry of Environment and Sustainable Development in Madagascar (N_025/23/MEDD/SG/DGGE/DAPRNE/SCBE.Re) and the Ministry of Environment, Climate Change and Forestry in Kenya (RESEA/1/KFS 98 and RESEA/1/KFS 22) for providing research permits, staff at A, BM, E, G, K, MO, P, PE, PRE, TAN, and US for the provision of loans and access to specimens, and Jin-Dan Zhang and Xiu-Ping Xu from the Plant Science Facility of the Institute of Botany, Chinese Academy of Sciences for their technical assistance. We thank Rhian Smith for her valuable suggestions on finalizing the title of this manuscript. This study was supported by the National Natural Science Foundation of China (32221001, 32270230), the National Key Research Development Program of China (2022YFC2601200, 2023YFF0805800), the International Partnership Program of CAS (063GJHZ2024053FN, 151853 KYSB20190027), the Youth Innovation Promotion Association CAS (2020080), and the Sino-Africa Joint Research Center, CAS International Research and Education Development Program (SAJC202527ZD01). AA and RLB acknowledge support from the Chinese Academy of Sciences President's International Fellowship Initiative. AA further acknowledges funding from the Swedish Research Council (2024-04303), the Swedish Foundation for Strategic Environmental Research MISTRA (Project BioPath), and the Kew Foundation. Rindra M. Ranaivoson and Romer N. Rabarijaona were supported by the CAS-TWAS President's Fellowship for International Ph.D. Students.

CONFLICTS OF INTEREST

The authors declare no conflicts of interest.

AUTHOR CONTRIBUTIONS

L.-M.L. and Z.-D.C. designed the study. R.M.R., R.N.R., J.-R.Y., Y.-C.Y., and D.-M.Z. conceived the Methodology. R.M.R., R.N.R., and L.-M.L. investigated the study. R.M.R., R.N.R., and L.-M.L. wrote the original draft. J.-R.Y., Y.-C.Y., R.L.B., J.Z., W.O.O., C.-Y.D., M.R., J.C., C.-B.L., Y.D., I.J.L., A.A., J.W., and Z.-D.C. reviewed and edited the article. Z.-D.C. and L.-M.L. acquired funds; All authors read and approved the paper.

Edited by: Bao Liu, Northeast Normal University in Changchun, China

Received Jun. 15, 2025; **Accepted** Nov. 20, 2025; **Published** Jan. 9, 2026

OO: OnlineOpen

REFERENCES

Akaike, H. (1974). A new look at the statistical model identification. IEEE Trans. Autom. Control **19:** 716–723.

Antonelli, A., Smith, R.J., Perrigo, A.L., Crottini, A., Hackel, J., Testo, W., Farooq, H., Torres Jiménez, M.F., Andela, N., Andermann, T., et al. (2022). Madagascar's extraordinary biodiversity: Evolution, distribution, and use. Science **378:** eabf0869.

Arakaki, M., Christin, P.-A., Nyffeler, R., Lendel, A., Eggli, U., Ogburn, R.M., Spriggs, E., Moore, M.J., and Edwards, E.J. (2011). Contemporaneous and recent radiations of the world's major succulent plant lineages. Proc. Natl. Acad. Sci. U.S.A. **108:** 8379–8384.

Beatriz, M., Folk, R.A., Grady, C.J., Spoelhof, J.P., Smith, S.A., Soltis, D.E., and Soltis, P.S. (2021). Is the age of plant communities predicted by the age, stability and soil composition of the underlying landscapes? An investigation of OCBILs. Biol. J. Linn. Soc. **133:** 297–316.

Beaulieu, J.M., Leitch, I.J., Patel, S., Pendharkar, A., and Knight, C.A. (2008). Genome size is a strong predictor of cell size and stomatal density in angiosperms. New Phytol. **179:** 975–986.

Bennett, M.D. (1971). The duration of meiosis. Proc. R. Soc. Lond. B Biol. Sci. **178:** 277–299.

Bilinski, P., Albert, P.S., Berg, J.J., Birchler, J.A., Grote, M.N., Lorant, A., Quezada, J., Swarts, K., Yang, J., and Ross-Ibarra, J. (2018). Parallel altitudinal clines reveal trends in adaptive evolution of genome size in *Zea mays*. PLoS Genet. **14:** e1007162.

Blomberg, S.P., Garland, T., and Ives, A.R. (2003). Testing for phylogenetic signal in comparative data: Behavioral traits are more labile. Evolution **57:** 717–745.

Bomblies, K. (2020). When everything changes at once: Finding a new normal after genome duplication. Proc. R. Soc. Lond. B Biol. Sci **287:** 20202154.

Buerki, S., Devey, D.S., Callmander, M.W., Phillipson, P.B., and Forest, F. (2013). Spatio-temporal history of the endemic genera of Madagascar. Bot. J. Linn. Soc. **171:** 304–329.

Bureš, P., Elliott, T.L., Veselý, P., Šmarda, P., Forest, F., Leitch, I.J., Lughadha, E.N., Soto Gomez, M., Pironon, S., Brown, M.J.M., et al. (2024). The global distribution of angiosperm genome size is shaped by climate. New Phytol. **242:** 744–759.

Burgette, L.F., and Reiter, J.P. (2010). Multiple imputation for missing data via sequential regression trees. Am. J. Epidemiol. **172:** 1070–1076.

Carta, A., Bedini, G., and Peruzzi, L. (2020). A deep dive into the ancestral chromosome number and genome size of flowering plants. New Phytol. **228:** 1097–1106.

Casacuberta, E., and González, J. (2013). The impact of transposable elements in environmental adaptation. Mol. Ecol. **22:** 1503–1517.

Cerling, T.E., Harris, J.M., MacFadden, B.J., Leakey, M.G., Quade, J., Eisenmann, V., and Ehleringer, J.R. (1997). Global vegetation change through the Miocene/Pliocene boundary. Nature **389:** 153–158.

Chazot, N., Condamine, F.L., Dudas, G., Peña, C., Kodandaramaiah, U., Matos-Maraví, P., Aduse-Poku, K., Elias, M., Warren, A.D., Lohman, D.J., et al. (2021). Conserved ancestral tropical niche but different continental histories explain the latitudinal diversity gradient in brush-footed butterflies. Nat. Commun. **12:** 5717.

Chamberlain, S., Oldoni, D., and Waller, J. (2022). Rgbif: Interface to the global biodiversity information facility API. Available from: https://cran.r-project.org/web/packages/rgbif/index.html.

Chen, I., and Manchester, S.R. (2007). Seed morphology of modern and fossil *Ampelocissus* (Vitaceae) and implications for phytogeography. Am. J. Bot. **94:** 1534–1553.

Chu, Z.F., Wen, J., Yang, Y.P., Nie, Z.L., and Meng, Y. (2018). Genome size variation and evolution in the grape family Vitaceae. J. Syst. Evol. **56:** 273–282.

Couvreur, T.L.P., Dauby, G., Blach-Overgaard, A., Deblauwe, V., Dessein, S., Droissart, V., Hardy, O.J., Harris, D.J., Janssens, S.B., Ley, A.C., et al. (2021). Tectonics, climate and the diversification of the tropical African terrestrial flora and fauna. Biol. Rev. **96:** 16–51.

De Rocher, E.J., Harkins, K.R., Galbraith, D.W., and Bohnert, H.J. (1990). Developmentally regulated systemic endopolyploid in succulents with small genomes. Science **250:** 99–101.

Devos, K.M., Brown, J.K.M., and Bennetzen, J.L. (2002). Genome size reduction through illegitimate recombination counteracts genome expansion in *Arabidopsis*. Genome Res. **12:** 1075–1079.

Dodsworth, S., Chase, M.W., and Leitch, A.R. (2016). Is post-polyploidization diploidization the key to the evolutionary success of angiosperms? Bot. J. Linn. Soc. **180:** 1–5.

Doležel, J., Greilhuber, J., and Suda, J. (2007). Estimation of nuclear DNA content in plants using flow cytometry. Nat. Protoc. **2:** 2233–2244.

Dong, S.S., Wang, Y.L., Xia, N.H., Liu, Y., Liu, M., Lian, L., Li, N., Li, L.F., Lang, X.A., Gong, Y.Q., et al. (2022). Plastid and nuclear phylogenomic incongruences and biogeographic implications of *Magnolia s.l.* (Magnoliaceae). J. Syst. Evol. **60:** 1–15.

Ebadi, M., Bafort, Q., Mizrachi, E., Audenaert, P., Simoens, P., Van Montagu, M., Bonte, D., and Van de Peer, Y. (2023). The duplication of genomes and genetic networks and its potential for evolutionary adaptation and survival during environmental turmoil. Proc. Natl. Acad. Sci. U. S. A. **120:** e2307289120.

Escudero, M., and Wendel, J.F. (2020). The grand sweep of chromosomal evolution in angiosperms. New Phytol. **228:** 805–808.

Evans, M., Aubriot, X., Hearn, D., Lanciaux, M., Lavergne, S., Cruaud, C., Lowry, P.P., and Haevermans, T. (2014). Insights on the evolution of plant succulence from a remarkable radiation in Madagascar (*Euphorbia*). Syst. Biol. **63:** 697–711.

Faizullah, L., Morton, J.A., Hersch-Green, E.I., Walczyk, A.M., Leitch, A.R., and Leitch, I.J. (2021). Exploring environmental selection on genome size in angiosperms. Trends Plant Sci. **26:** 1039–1049.

Fleischmann, A., Michael, T.P., Rivadavia, F., Sousa, A., Wang, W., Temsch, E.M., Greilhuber, J., Müller, K.F., and Heubl, G. (2014). Evolution of genome size and chromosome number in the carnivorous plant genus *Genlisea* (Lentibulariaceae), with a new estimate of the minimum genome size in angiosperms. Ann. Bot. **114:** 1651–1663.

FitzJohn, R.G. (2012). Diversitree: Comparative phylogenetic analyses of diversification in R. Methods Ecol. Evol. **3:** 1084–1092.

Flörchinger, M., Braun, J., Böhning-Gaese, K., and Schaefer, H.M. (2010). Fruit size, crop mass, and plant height explain differential fruit choice of primates and birds. Oecologia **164:** 151–161.

Flügel, E. (2010) *Microfacies of carbonate rocks: Analysis, interpretation and application*. 2nd ed. Springer, Berlin, Germany.

Galbraith, D.W., Harkins, K.R., Maddox, J.M., Ayres, N.M., Sharma, D.P., and Firoozabady, E. (1983). Rapid flow cytometric analysis of the cell cycle in intact plant tissues. Science **220:** 1049–1051.

Gilman, I.S., Smith, J.A.C., Holtum, J.A.M., Sage, R.F., Silvera, K., Winter, K., and Edwards, E.J. (2023). The CAM lineages of planet Earth. Ann. Bot. **132:** 627–654.

Good-Avila, S.V., Souza, V., Gaut, B.S., and Eguiarte, L.E. (2006). Timing and rate of speciation in *Agave* (Agavaceae). Proc. Natl. Acad. Sci. U. S. A. **103:** 9124–9129.

Griffiths, H., and Males, J. (2017). Succulent plants. Curr. Biol. **27:** R890–R896.

Guignard, M.S., Crawley, M.J., Kovalenko, D., Nichols, R.A., Trimmer, M., Leitch, A.R., and Leitch, I.J. (2019). Interactions between plant genome size, nutrients and herbivory by rabbits, molluscs and insects on a temperate grassland. Proc. R. Soc. Lond. B Biol. Sci. **286:** 20182619.

Guignard, M.S., Nichols, R.A., Knell, R.J., Macdonald, A., Romila, C.-A., Trimmer, M., Leitch, I.J., and Leitch, A.R. (2016). Genome size and ploidy influence angiosperm species' biomass under nitrogen and phosphorus limitation. New Phytol. **210:** 1195–1206.

Guo, K., Pyšek, P., van Kleunen, M., Kinlock, N.L., Lučanová, M., Leitch, I.J., Pierce, S., Dawson, W., Essl, F., Kreft, H., et al. (2024). Plant invasion and naturalization are influenced by genome size, ecology and economic use globally. Nat. Commun. **15:** 1330.

Hearn, D.J., Evans, M., Wolf, B., McGinty, M., and Wen, J. (2018). Dispersal is associated with morphological innovation, but not increased diversification, in *Cyphostemma* (Vitaceae). J. Syst. Evol. **56:** 340–359.

Hedges, S.B. (1992). The number of replications needed for accurate estimation of the bootstrap P value in phylogenetic studies. Mol. Biol. Evol. **9:** 366–369.

Henniges, M.C., Johnston, E., Pellicer, J., Hidalgo, O., Bennett, M.D., and Leitch, I.J. (2023). The Plant DNA C-values database: A one-stop shop for plant genome size data. In Plant genomic and cytogenetic databases. In *Methods in Molecular Biology*. Garcia, S., Nualart, N., eds, (New York: Humana Press), pp. 111–122.

Hetherington, A., and Woodward, F. (2003). The role of stomata in sensing and driving environmental change. Nature **424:** 901–908.

Hiremath, S., Chinnappa, C. (2015). Plant chromosome preparations and staining for light microscopic studies. In *Plant microtechniques and protocols*. Yeung, E., Stasolla, C., Sumner, M., Huang, B., eds, (Cham: Springer), pp. 263–286.

Hopper, S.D., Lambers, H., Fiedler, P.L., and Silviera, F.A.O. (2021). OCBIL theory examined: Reassessing evolution, ecology, and conservation in the world's ancient, climatically buffered and infertile landscapes. Biol. J. Linn. Soc. **133:** 266–296.

Jin, Y., and Qian, H. (2019). V.PhyloMaker: An R package that can generate very large phylogenies for vascular plants. Ecography **42:** 1353–1359.

Jin, J.J., Yu, W.B., Yang, J.B., Song, Y., dePamphilis, C.W., Yi, T.S., and Li, D.Z. (2020). GetOrganelle: A fast and versatile toolkit for accurate de novo assembly of organelle genomes. Genome Biol. **21:** 241.

Johnson, M.G., Gardner, E.M., Liu, Y., Medina, R., Goffinet, B., Shaw, A.J., Zerega, N.J.C., and Wickett, N.J. (2016). HybPiper: Extracting coding sequence and introns for phylogenetics from high-throughput sequencing reads using target enrichment. Appl. Plant Sci. **4:** 1600016.

Jønsson, K.A., Fabre, P.H., Fritz, S.A., Etienne, R.S., Ricklefs, R.E., Jørgensen, T.B., Fjeldså, J., Rahbek, C., Ericson, P.G., Woog, F., et al. (2012). Ecological and evolutionary determinants for the adaptive radiation of the Madagascan vangas. Proc. Natl. Acad. Sci. U. S. A. **109:** 6620–6625.

Kang, H., Smith, J.A.C., Lee, W.G., and Edwards, E.J. (2015). Nitrogen limitation as a driver of genome size evolution in plants. New Phytol. **206:** 558–567.

Kassambara, A. (2022). rstatix: Pipe-friendly framework for basic statistical tests. R package version 0.7.1. Available at: https://github.com/kassambara/rstatix

Kearse, M., Moir, R., Wilson, A., Stones-Havas, S., Cheung, M., Sturrock, S., Buxton, S., Cooper, A., Markowitz, S., Duran, C., et al. (2012). Geneious Basic: An integrated and extendable desktop software platform for the organization and analysis of sequence data. Bioinformatics **28:** 1647–1649.

Kim, W., Schmidt, N., Jost, M., Mkala, E.M., Winkler, S., Hu, G., Heitkam, T., and Wanke, S. (2025). Diverging repeatomes in holoparasitic Hydnoraceae uncover a playground of genome evolution. New Phytol. **247:** 1520–1537.

Knight, C.A., Molinari, N.A., and Petrov, D.A. (2005). The large genome constraint hypothesis: Evolution, ecology and phenotype. Ann. Bot. **95:** 177–190.

Landis, J.B., Soltis, D.E., Li, Z., Marx, H.E., Barker, M.S., Tank, D.C., and Soltis, P.S. (2018). Impact of whole-genome duplication events on diversification rates in angiosperms. Am. J. Bot. **105:** 348–363.

Lavie, P. (1979). Caryosystematique des Vitaceae. 1: *Cissus* L., *Cyphostemma* (Planch.) Alst., *Rhoicissus* Planch. Adansonia **19:** 175–198.

Leitch, A.R., and Leitch, I.J. (2022). Genome evolution: On the nature of trade-offs with polyploidy and endopolyploidy. Curr. Biol. **32:** R952–R954.

Leitch, I.J., Chase, M.W., and Bennett, M.D. (1998). Phylogenetic analysis of DNA C-values provides evidence for a small ancestral genome size in flowering plants. Ann. Bot. **82:** 85–94.

Li, Q., Wang, Y., Zhou, H., Liu, Y., Gichuki, D.K., Hou, Y., Zhang, J., Aryal, R., Hu, G., Wan, T., et al. (2024). The *Cissus quadrangularis* genome reveals its adaptive features in an arid habitat. Hortic. Res. **11:** uhae038.

Lichter-Marck, I.H., and Baldwin, B.G. (2023). Edaphic specialization onto bare, rocky outcrops as a factor in the evolution of desert angiosperms. Proc. Natl. Acad. Sci. U. S. A. **120:** e2214729120.

Losos, J.B., Mahler, D.L. (2010). Adaptive radiation: The interaction of ecological opportunity, adaptation, and speciation. In *Evolution since Darwin: The first 150 years*. Bell, M.A., Futuyma, D.J., Eanes, W.F., Levinton, J.S., eds, (Oxford, UK: Oxford University Press), pp. 281–420.

Loureiro, J., Rodriguez, E., Doležel, J., and Santos, C. (2006). Comparison of four nuclear isolation buffers for plant DNA flow cytometry. Ann. Bot. **98:** 679–689.

Lu, L.M., Wang, W., Chen, Z.D., and Wen, J. (2013). Phylogeny of the non-monophyletic *Cayratia* Juss. (Vitaceae) and implications for character evolution and biogeography. Mol. Phylogenet. Evol. **68:** 502–515.

Magallón, S., and Castillo, A. (2009). Angiosperm diversification through time. Am. J. Bot. **96:** 349–365.

Matzke, N.J. (2012). Founder-event speciation in BioGeoBEARS package dramatically improves likelihoods and alters parameter inference in Dispersal-Extinction-Cladogenesis (DEC) analyses. Front. Biogeogr. **4:** 210.

Matzke, N.J. (2014). Model selection in historical biogeography reveals that founder-event speciation is a crucial process in island clades. Syst. Biol. **63:** 951–970.

Meudt, H.M., Albach, D.C., Tanentzap, A.J., Igea, J., Newmarch, S.C., Brandt, A.J., Lee, W.G., and Tate, J.A. (2021). Polyploidy on islands: Its emergence and importance for diversification. Front. Plant Sci. **12:** 637214.

Miller, M.A., Pfeiffer, W., Schwartz, T. (2010). Creating the CIPRES Science Gateway for inference of large phylogenetic trees. In *2010 Gateway Computing Environments Workshop (GCE)*. (New Orleans, LA: IEEE), pp. 1–8.

Mirarab, S., Reaz, R., Bayzid, M.S., Zimmermann, T., Swenson, M.S., and Warnow, T. (2014). ASTRAL: Genome-scale coalescent-based species tree estimation. Bioinformatics **30:** i541–i548.

Morlon, H., Schwilk, D.W., Bryant, J.A., Marquet, P.A., Rebelo, A.G., Tauss, C., Bohannan, B.J.M., and Green, J.L. (2016). RPANDA: An R package for macroevolutionary analyses on phylogenetic trees. Methods Ecol. Evol **7:** 589–597.

Morton, J.A., Arnillas, C.A., Biedermann, L., Borer, E.T., Brudvig, L.A., Buckley, Y.M., Cadotte, M.W., Davies, K., Donohue, I., Ebeling, A., et al. (2024). Genome size influences plant growth and biodiversity responses to nutrient fertilization in diverse grassland communities. PLoS Biol. **22:** e3002927.

Mucina, L., Lötter, M.C., Rutherford, M.C., van Niekerk, A., Macintyre, P.D., Tsakalos, J.L., Timberlake, J., Adams, J.B., Riddin, T., and McCarthy, L.K. (2021). Forest biomes of Southern Africa. N.Z. J. Bot **60:** 377–428.

Nevo, E. (2001). Evolution of genome-phenome diversity under environmental stress. Proc. Natl. Acad. Sci. U. S. A. **98:** 6233–6240.

Nguyen, L.T., Schmidt, H.A., von Haeseler, A., and Minh, B.Q. (2015). IQ-TREE: A fast and effective stochastic algorithm for estimating maximum-likelihood phylogenies. Mol. Biol. Evol. **32:** 268–274.

Nie, Z.L., Hodel, R., Ma, Z.Y., Johnson, G., Ren, C., Meng, Y., Ickert-Bond, S.M., Liu, X.Q., Zimmer, E., and Wen, J. (2023). Climate-influenced boreotropical survival and rampant introgressions explain the thriving of New World grapes in the north temperate zone. J. Integr. Plant Biol. **65:** 1183–1203.

Nilsson, S., Coetzee, J., and Grafström, E. (1996). On the origin of the Sarcolaenaceae with reference to pollen morphological evidence. Grana **35:** 321–334.

Novák, P., Guignard, M.S., Neumann, P., Kelly, L.J., Mlinarec, J., Koblížková, A., Dodsworth, S., Kovařík, A., Pellicer, J., Wang, W., et al. (2020). Repeat-sequence turnover shifts fundamentally in species with large genomes. Nat. Plants **6:** 1335–1341.

Ohri, D. (2005). Climate and growth form: The consequences for genome size in plants. Plant Biol. **7:** 449–458.

Okuyama, Y., Fujii, N., Wakabayashi, M., Kawakita, A., Ito, M., Watanabe, M., Murakami, N., and Kato, M. (2005). Nonuniform concerted evolution and chloroplast capture: Heterogeneity of observed introgression patterns in three molecular data partition phylogenies of Asian *Mitella* (Saxifragaceae). Mol. Biol. Evol. **22:** 285–296.

Omollo, W.O., Rabarijaona, R.N., Ranaivoson, R.M., Rakotoarinivo, M., Barrett, R.L., Zhang, Q., Lai, Y.-J., Ye, J.F., Le, C.T., Antonelli, A., et al. (2024). Spatial heterogeneity of neo- and paleo-endemism for plants in Madagascar. Curr. Biol. **34:** 1271–1283.

Orme, D., Freckleton, R., Thomas, G., Petzoldt, T., Fritz, S., Isaac, N., and Pearse, W. (2013). *The caper package: Comparative analyses of phylogenetics and evolution in R*. R package version 0.5.2. 1–36 Available at: https://cran.r-project.org/web/packages/caper/index.html.

Pacey, E.K., Maherali, H., and Husband, B.C. (2022). Polyploidy increases storage but decreases structural stability in *Arabidopsis thaliana*. Curr. Biol. **32:** 4057–4063.

Pagel, M. (1999). Inferring the historical patterns of biological evolution. Nature **401:** 877–884.

Paradis, E., Claude, J., and Strimmer, K. (2004). APE: Analyses of phylogenetics and evolution in R language. Bioinformatics **20:** 289–290.

Peel, M.C., Finlayson, B.L., and McMahon, T.A. (2007). Updated world map of the Köppen-Geiger climate classification. Hydrol. Earth Syst. Sci. **11:** 1633–1644.

Pellicer, J., and Leitch, I.J. (2020). The Plant DNA C-values database (release 7.1): An updated online repository of plant genome size data for comparative studies. New Phytol. **226:** 301–305.

Pellicer, J., Fay, M.F., and Leitch, I.J. (2010). The largest eukaryotic genome of them all? Bot. J. Linn. Soc. **164:** 10–15.

Peng, Y., Yang, J., Leitch, I.J., Guignard, M.S., Seabloom, E.W., Cao, D., Zhao, F., Li, H., Han, X., Jiang, Y., et al. (2022). Plant genome size modulates grassland community responses to multi-nutrient additions. New Phytol. **236:** 2091–2102.

Pennell, M.W., Eastman, J.M., Slater, G.J., Brown, J.W., Uyeda, J.C., FitzJohn, R.G., Alfaro, M.E., and Harmon, L.J. (2014). geiger v2.0: An expanded suite of methods for fitting macroevolutionary models to phylogenetic trees. Bioinformatics **30:** 2216–2218.

Pinheiro, J., Bates, D., DebRoy, S., Sarkar, D., and R Core Team. (2021). *nlme: Linear and nonlinear mixed effects models*. Vienna, Austria: R Foundation for Statistical Computing. Available at: https://CRAN.R-project.org/package=nlme.

Pokorny, L., Riina, R., Mairal, M., Meseguer, A.S., Culshaw, V., Cendoya, J., Serrano, M., Carbajal, R., Ortiz, S., Heuertz, M., et al. (2015). Living on the edge: Timing of Rand Flora disjunctions congruent with ongoing aridification in Africa. Front. Genet. **6:** 154.

Powell, R.F., Pulido Suarez, L., Magee, A.R., Boatwright, J.S., Kapralov, M.V., and Young, A.J. (2020). Genome size variation and endopolyploidy in the diverse succulent plant family Aizoaceae. Bot. J. Linn. Soc. **194:** 47–68.

Pyšek, P., Lučanová, M., Dawson, W., Essl, F., Kreft, H., Leitch, I.J., Lenzner, B., Meyerson, L.A., Pergl, J., van Kleunen, M., et al. (2023). Small genome size and variation in ploidy levels support the naturalization of vascular plants but constrain their invasive spread. New Phytol. **239:** 2389–2403.

Rabarijaona, R.N., Ranaivoson, R.M., Yu, J.R., You, Y.C., Liu, B., Ye, J.F., Barrett, R.L., Rakotoarinivo, M., Lin, X.L., Wen, J., et al. (2023). Species delimitation and biogeography of *Cyphostemma* (Vitaceae), emphasizing diversification and ecological adaptation in Madagascar. Taxon **72:** 766–790.

Rabarijaona, R.N., Yu, J.R., Tang, Z.Y., Ranaivoson, R.M., Barrett, R.L., Rakotoarinivo, M., Liu, B., You, Y.C., Yaradua, S.S., Gbiribou, R., et al. (2025). Phylogenomic insights into historical biogeography and species delimitation of African *Ampelocissus* (Vitaceae). Mol. Phylogenet. Evol. **211:** 108388.

Rabinowitz, P.D., Coffin, M.F., and Falvey, D. (1983). The separation of Madagascar and Africa. Science **220:** 67–69.

Rabosky, D.L., Santini, F., Eastman, J., Smith, S.A., Sidlauskas, B., Chang, J., and Alfaro, M.E. (2014). BAMMtools: An R package for the analysis of evolutionary dynamics on phylogenetic trees. Methods Ecol. Evol **5:** 701–707.

Rambaut, A., Drummond, A.J., Xie, D., Baele, G., and Suchard, M.A. (2018). Posterior summarisation in Bayesian phylogenetics using Tracer 1.7. Syst. Biol. **67:** 901–904.

Razafimandimbison, S.G., Kainulainen, K., Wikström, N., and Bremer, B. (2017). Historical biogeography and phylogeny of the pantropical Psychotrieae alliance (Rubiaceae), with particular emphasis on the Western Indian Ocean Region. Am. J. Bot. **104:** 1407–1423.

Razafimandimbison, S.G., Taylor, C.M., Wikstrom, N., Pailler, T., Khodabandeh, A., and Bremer, B. (2014). Phylogeny and generic limits in the sister tribes Psychotrieae and Palicoureeae (Rubiaceae): Evolution of schizocarps in *Psychotria* and origins of bacterial leaf nodules in the Malagasy species. Am. J. Bot. **101:** 1102–1126.

Revell, L.J. (2012). Phytools: An R package for phylogenetic comparative biology (and other things). Methods Ecol. Evol **3:** 217–223.

Roddy, A.B., Théroux-Rancourt, G., Abbo, T., Benedetti, J.W., Brodersen, C.R., Castro, M., Castro, S., Gilbride, A.B., Jensen, B., Jiang, G.F., et al. (2020). The scaling of genome size and cell size limits maximum rates of photosynthesis with implications for ecological strategies. Int. J. Plant Sci. **181:** 75–87.

Rodewald, S.E., Klein, D.P., Shtein, R., Smith, G.F., Joyce, E.M., Morales-Briones, D.F., Bernhard, S., Letsara, R., Mertes, H., Hühn, P., et al. (2025). A new phylogenetic framework for the genus *Kalanchoe* (Crassulaceae) and implications for infrageneric classification. Ann. Bot. **135:** 1311–1328.

Sage, R.F., Gilman, I.S., Smith, J.A.C., Silvera, K., and Edwards, E.J. (2023). Atmospheric CO_2 decline and the timing of CAM plant evolution. Ann. Bot. **132:** 753–770.

Schubert, I., and Vu, G.T.H. (2016). Genome stability and evolution: Attempting a holistic view. Trends Plant Sci. **21:** 749–757.

Sepulchre, P., Ramstein, G., Fluteau, F., Schuster, M., Tiercelin, J.J., and Brunet, M. (2006). Tectonic uplift and Eastern Africa aridification. Science **313:** 1419–1423.

Shah, A.D., Bartlett, J.W., Carpenter, J., Nicholas, O., and Hemingway, H. (2014). Comparison of random forest and parametric imputation models for imputing missing data using MICE: A CALIBER study. Am. J. Epidemiol. **179:** 764–774.

Sharrow, S.O. (2002). Overview of flow cytometry. Curr. Protoc. Immunol. **50:** 5.1.1–5.1.8.

Simonin, K.A., Roddy, A.B. (2018) Genome downsizing, physiological novelty, and the global dominance of flowering plants. PLoS Biol. **16:** e2003706.

Šímová, I., and Herben, T. (2012). Geometrical constraints in the scaling relationships between genome size, cell size and cell cycle length in herbaceous plants. Proc. R. Soc. Lond. B Biol. Sci. **279:** 867–875.

Simpson, K.J., Mian, S., Forrestel, E.J., Hackel, J., Morton, J.A., Leitch, A.R., and Leitch, I.J. (2024). Bigger genomes provide environment-dependent growth benefits in grasses. New Phytol. **244:** 2049–2061.

Sinha, S., Nair, R.R., Sinha, R.K. (2016). Preparation of mitotic and meiotic metaphase chromosomes from young leaves and flower buds of *Coccinia grandis*. Bio Protoc. **6:** e1771.

Šmarda, P., Klem, K., Knápek, O., Veselá, B., Veselá, K., Holub, P., Kuchař, V., Šilerová, A., Horová, L., and Bureš, P. (2023). Growth, physiology, and stomatal parameters of plant polyploids grown under ice age, present-day, and future CO_2 concentrations. New Phytol. **239:** 399–414.

Soto Gomez, M., Brown, M.J.M., Pironon, S., Bureš, P., Verde Arregoitia, L.D., Veselý, P., Elliott, T.L., Zedek, F., Pellicer, J., Forest, F., et al. (2024). Genome size is positively correlated with extinction risk in herbaceous angiosperms. New Phytol. **243:** 2470–2485.

Théroux-Rancourt, G., Roddy, A.B., Earles, J.M., Gilbert, M.E., Zwieniecki, M.A., Boyce, C.K., Tholen, D., McElrone, A.J., Simonin, K.A., and Brodersen, C.R. (2021). Maximum CO_2 diffusion inside leaves is limited by the scaling of cell size and genome size. Proc. R. Soc. Lond. B Biol. Sci. **288:** 20203145.

Tillich, M., Lehwark, P., Pellizzer, T., Ulbricht-Jones, E.S., Fischer, A., Bock, R., and Greiner, S. (2017). GeSeq–versatile and accurate annotation of organelle genomes. Nucleic Acids Res. **45:** W6–W11.

Van de Peer, Y., Ashman, T.L., Soltis, P.S., and Soltis, D.E. (2021). Polyploidy: An evolutionary and ecological force in stressful times. Plant Cell **33:** 11–26.

Van Mazijk, R., West, A.G., Verboom, G.A., Elliott, T.L., Bureš, P., and Muasya, A.M. (2024). Genome size variation in Cape schoenoid sedges (Schoeneae) and its ecophysiological consequences. Am. J. Bot. **111:** e16315.

Verboom, A.G., Archibald, J.K., Bakker, F.T., Bellstedt, D.U., Conrad, F., Dreyer, L.L., Forest, F., Galley, C., Goldblatt, P., Henning, J.F., et al. (2009). Origin and diversification of the Greater Cape flora: Ancient species repository, hot-bed of recent radiation, or both? Mol. Phylogenet. Evol. **51:** 44–53.

Veselý, P., Šmarda, P., Bureš, P., Stirton, C., Muasya, A.M., Mucina, L., Horová, L., Veselá, K., Šilerová, A., Šmerda, J., et al. (2020). Environmental pressures on stomatal size may drive plant genome size evolution: Evidence from a natural experiment with Cape geophytes. Ann. Bot. **126:** 323–330.

Virzo De Santo, A., Alfani, A., Russo, G., and Fioretto, A. (1983). Relationship between CAM and succulence in some species of Vitaceae and Piperaceae. Bot. Gaz. **144:** 342–346.

Wang, X., Morton, J.A., Pellicer, J., Leitch, I.J., and Leitch, A.R. (2021). Genome downsizing after polyploidy: Mechanisms, rates and selection pressures. Plant J. **107:** 1003–1015.

Wen, J., Lu, L.M., Nie, Z.L., Liu, X.Q., Zhang, N., Ickert-Bond, S., Gerrath, J., Manchester, S.R., Boggan, J., and Chen, Z.D. (2018). A new phylogenetic tribal classification of the grape family (Vitaceae). J. Syst. Evol. **56:** 262–272.

Wen, J., Xiong, Z., Nie, Z.L., Mao, L., Zhu, Y., Kan, X.Z., Ickert-Bond, S.M., Gerrath, J., Zimmer, E.A., and Fan, X.D. (2013). Transcriptome sequences resolve deep relationships of the grape family. PLoS ONE **8:** e74394.

Wendel, J.F. (2015). The wondrous cycles of polyploidy in plants. Am. J. Bot. **102:** 1753–1756.

Westerhold, T., Marwan, N., Drury, A.J., Liebrand, D., Agnini, C., Anagnostou, E., Barnet, J.S.K., Bohaty, S.M., De Vleeschouwer, D., Florindo, F., et al. (2020). An astronomically dated record of Earth's climate and its predictability over the last 66 million years. Science **369:** 1383–1387.

Wichura, H., Bousquet, R., Oberhänsli, R., Strecker, M.R., and Trauth, M.H. (2010). Evidence for middle Miocene uplift of the East African Plateau. Geology **38:** 543–546.

Yang, Z. (2007). PAML 4: Phylogenetic analysis by maximum likelihood. Mol. Biol. Evol. **24:** 1586–1591.

Yoder, A.D., and Nowak, M.D. (2006). Has vicariance or dispersal been the predominant biogeographic force in Madagascar? Only time will tell. Annual Rev. Ecol. Evol. Syst **37:** 405–431.

You, Y., Yu, J., Nie, Z., Peng, D., Barrett, R.L., Rabarijaona, R.N., Lai, Y., Zhao, Y., Dang, V.C., et al. (2024). Transition of survival strategies under global climate shifts in the grape family. Nat. Plants **10:** 1100–1111.

Yu, Y., Blair, C., and He, X. (2020). RASP 4: Ancestral state reconstruction tool for multiple genes and characters. Mol. Biol. Evol. **37:** 604–606.

Yu, J.R., Niu, Y.T., You, Y.C., Cox, C.J., Barrett, R.L., Trias-Blasi, A., Guo, J., Wen, J., Lu, L.M., and Chen, Z.D. (2023a). Integrated phylogenomic analyses unveil reticulate evolution in *Parthenocissus* (Vitaceae), highlighting speciation dynamics in the Himalayan-Hengduan Mountains. New Phytol. **238:** 888–903.

Yu, J.R., Zhao, H., Niu, Y.T., You, Y.C., Barrett, R.L., Ranaivoson, R.M., Rabarijaona, R.N., Parmar, G., Yuan, L.X., Jin, X.F., et al. (2023b). Distinct hybridization modes in wide- and narrow-ranged lineages of *Causonis* (Vitaceae). BMC Biol. **21:** 209.

Yule, G.U. (1925). A mathematical theory of evolution, based on the conclusions of Dr. J. C. Willis, F.R.S. Philos. Trans. R. Soc. Lond. B Biol. Sci. **213:** 21–87.

Zenil-Ferguson, R., Ponciano, J.M., and Burleigh, J.G. (2016). Evaluating the role of genome downsizing and size thresholds from genome size distributions in angiosperms. Am. J. Bot. **103:** 1175–1186.

Zhang, D.M. (1998). Systematics of the tribe Ophiopogoneae (Liliaceae s.l.) with special reference to karyotypes and chromosomal evolution. Cathaya **10:** 1–154.

Zhao, W.Y., Liu, Z.C., Shi, S., Li, J.L., Xu, K.W., Huang, K.Y., Chen, Z.H., Wang, Y.R., Huang, C.Y., Wang, Y., et al. (2024). Landform and lithospheric development contribute to the assembly of mountain floras in China. Nat. Commun. **15:** 5139.

SUPPORTING INFORMATION

Additional Supporting Information may be found online in the supporting information tab for this article: http://onlinelibrary.wiley.com/doi/10.1111/jipb.70111/suppinfo

Figure S1. Sampling locations (black dots) plotted on the species richness map of *Cyphostemma*
Figure S2. Topological comparison between plastid and nuclear-derived phylogenies
Figure S3. Time-calibrated phylogeny of *Cyphostemma* inferred from the 159-plastome dataset with a Bayesian analysis in BEAST
Figure S4. Time-calibrated phylogeny of *Cyphostemma* species inferred from a coalescent species tree of the 104taxa-229nu dataset using MCMCTree
Figure S5. Biogeographic reconstruction for *Cyphostemma* based on the dated phylogeny of 83taxa-229nu dataset
Figure S6. Diversification rate shifts within *Cyphostemma*
Figure S7. Posterior probability distributions for rates of speciation, net diversification, extinction, and transition for succulence, tendrils, aridity level, and habitat types
Figure S8. Ancestral state reconstructions of succulence and tendrils in *Cyphostemma*
Figure S9. Ancestral state reconstructions of leaf habit and tuberous roots in *Cyphostemma*
Figure S10. Ancestral state reconstructions of leaf architecture and trichomes in *Cyphostemma*
Figure S11. Ancestral state reconstructions of the life form and the stem base in *Cyphostemma*
Figure S12. Ancestral state reconstruction of habitat types in *Cyphostemma*
Figure S13. Histograms showing the fluorescence intensity of propidium iodide-stained nuclei from two individuals of *Cyphostemma* species measured by flow cytometry
Figure S14. Flow cytometry measurements comparing genome size methods
Figure S15. Photomicrographs of mitotic metaphase chromosomes for representative species of *Cyphostemma*
Figure S16. Correlation between the measured genome sizes and chromosome numbers (2*n*) across 25 *Cyphostemma* species
Figure S17. Boxplots showing genome size variation across habitat types and morphological traits in *Cyphostemma*
Figure S18. Genome size evolution in *Cyphostemma*
Figure S19. PGLS fit linear regression model showing relationships between genome size and bioclimatic variables identified as predictors for genome size variation in *Cyphostemma* species
Figure S20. Trait-dependent diversification analyses using BiSSE of *Cyphostemma* species with large genomes or small genomes
Figure S21. Genome size variation within eudicots in relation to biome types and parasitism states
Figure S22. Genome size variation across aridity levels and succulence in temperate versus tropical and subtropical eudicots
Table S1. Model test for biogeographic analyses using BioGeoBEARS implemented in RASP v.4.2 with and without j founder-event parameter
Table S2. Diversification dynamics and optimal model from MEDUSA of *Cyphostemma* and two major clades
Table S3. Best-fitting models of diversification selected with RPANDA (shown in bold)
Table S4. Strength and significance of phylogenetic signal for the eight morphological traits, habitat type, aridity level, and genome size according to a likelihood ratio test
Table S5. Model fit comparisons for BiSSE analyses
Table S6. Model fit comparisons for MuSSE analyses
Table S7. Genome sizes (1C-values) for 74 species of *Cyphostemma* estimated using flow cytometry
Table S8. Genome sizes (1C-values) for an additional 24 species of Vitaceae were estimated using flow cytometry
Table S9. List of reference standards used for the flow cytometry measurement of genome size in *Cyphostemma* and additional species of Vitaceae (Tables S7, S8)
Table S10. Selection of bioclimatic variable predictors (in bold) significantly related to the variation in genome size among *Cyphostemma* species
Table S11. Genome size, distribution, climate, aridity level, and succulent states for 5,713 species of eudicots
Table S12. Strength and significance of phylogenetic signal for genome size, aridity level, succulence, distribution, biome, and parasitism across 5,713 species of eudicots
Table S13. Vouchers and GenBank accession numbers for all Vitaceae samples used in this study

Table S14. Genome size, chromosome number, morphological traits, habitat types, aridity level, and bioclimatic variables for *Cyphostemma* species

Table S15. Genome size simulation (1C-values) for 38 *Cyphostemma* species without genome size measurements using the MICE R package